APPLICAZIONI DELLA TEORIA DELLA DECISIONE E DELLA STIMA

Fabrizio LOMBARDINI, Lucio VERRAZZANI

Pisa, 20 Dicembre 2007

http://www.ing.unipi.it/~d9263/

Sommario

- Array signal processing
- Stima spettrale in rumore moltiplicativo, a super-risoluzione, adattiva
- Stima spettrale spazio-temporale
- Interpolatori e filtri non stazionari
- Bound di Cramér-Rao e di Cramér-Rao ibridi
- Robust signal processing

- Interferometria SAR
- Tomografia radar 3D
- Imaging differenziale
- Studi di sistema per radar satellitari multicanale

Radar d'immagine (SAR, 2D)

SAR satellitare

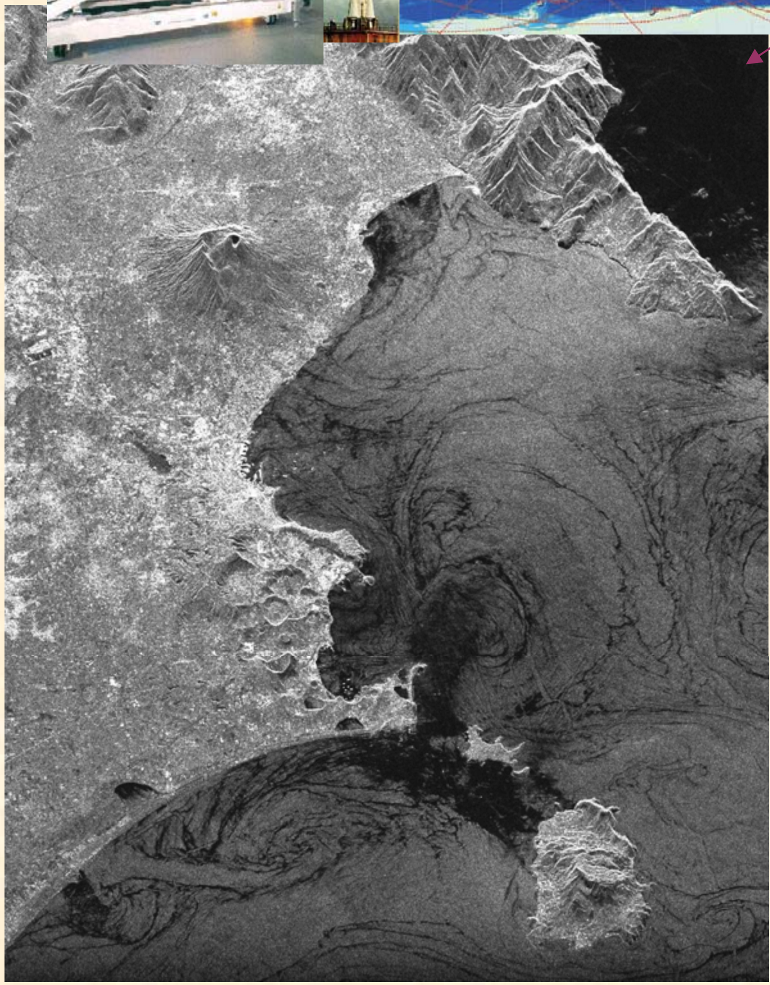

SAR aviotrasportato

M. Serra
CAPANNORI
SAN GIULIANO TERME
CALCI
Calci
Agnano
Montemagno
M. Cimone
Mezzana
Caprona
Campo
Colignola
Ripoli
CASCINA
Certosa di Pisa

Interferometria SAR – “2.5 D” !

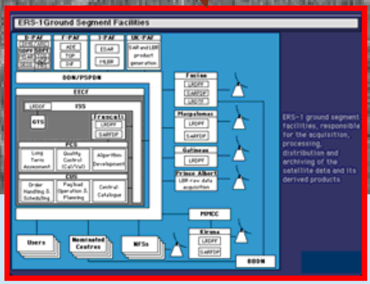

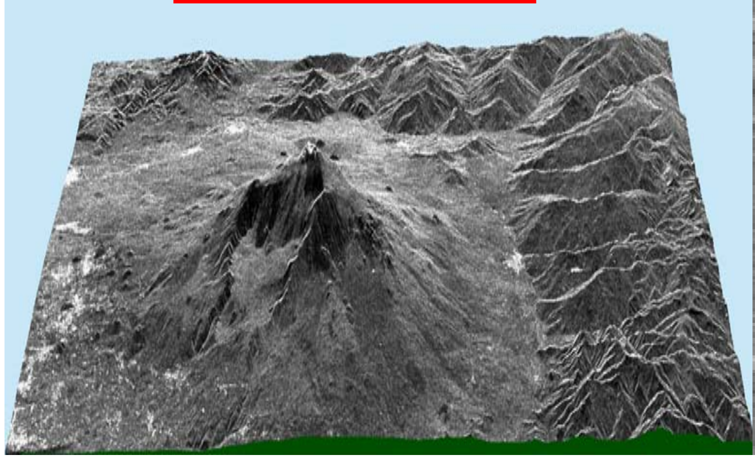

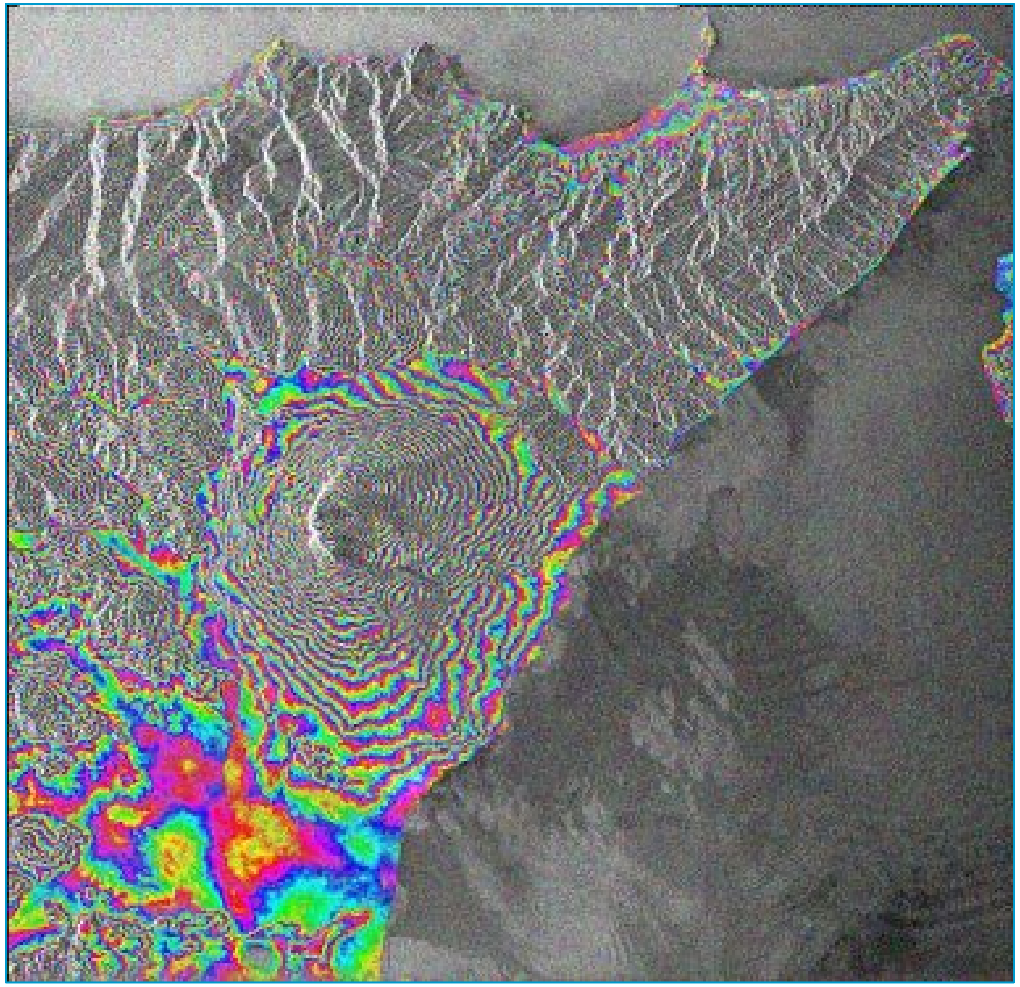

Etna, Sicilia
satellite europeo ERS-1/2

Interferometria SAR – 2D + T !

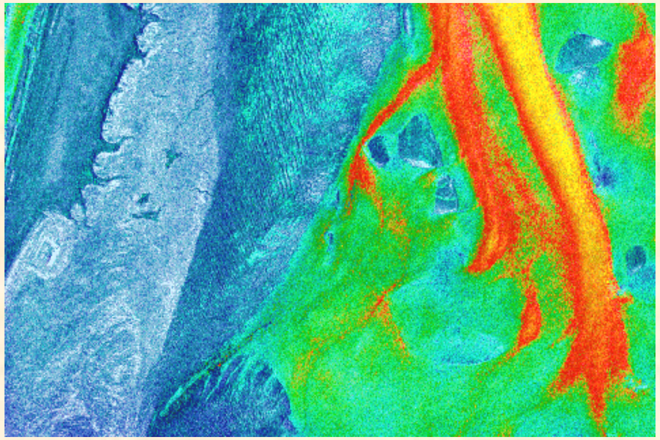

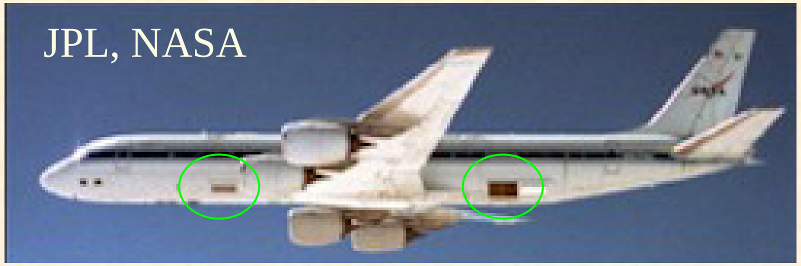

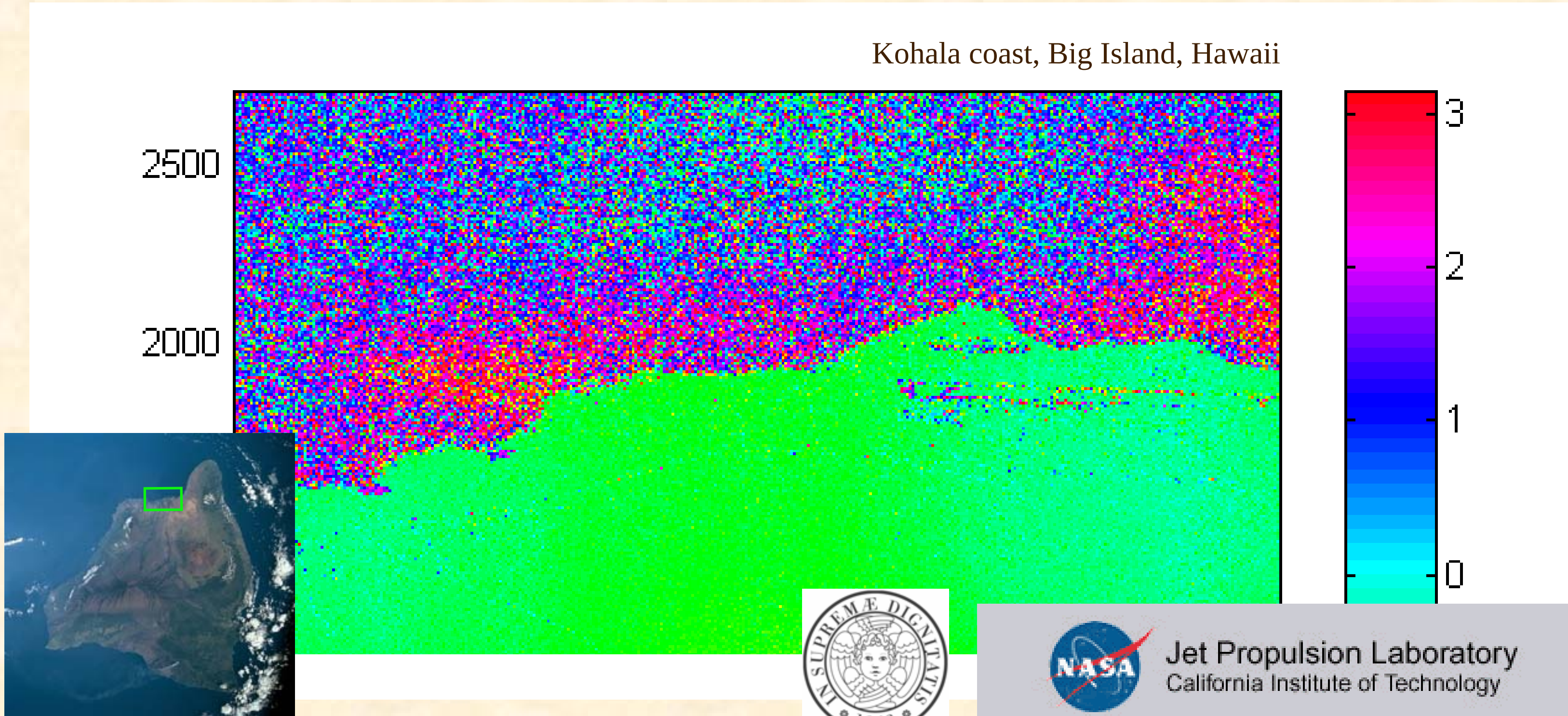

Jet Propulsion Laboratory
California Institute of Technology

Tecnica InSAR e ATI-SAR

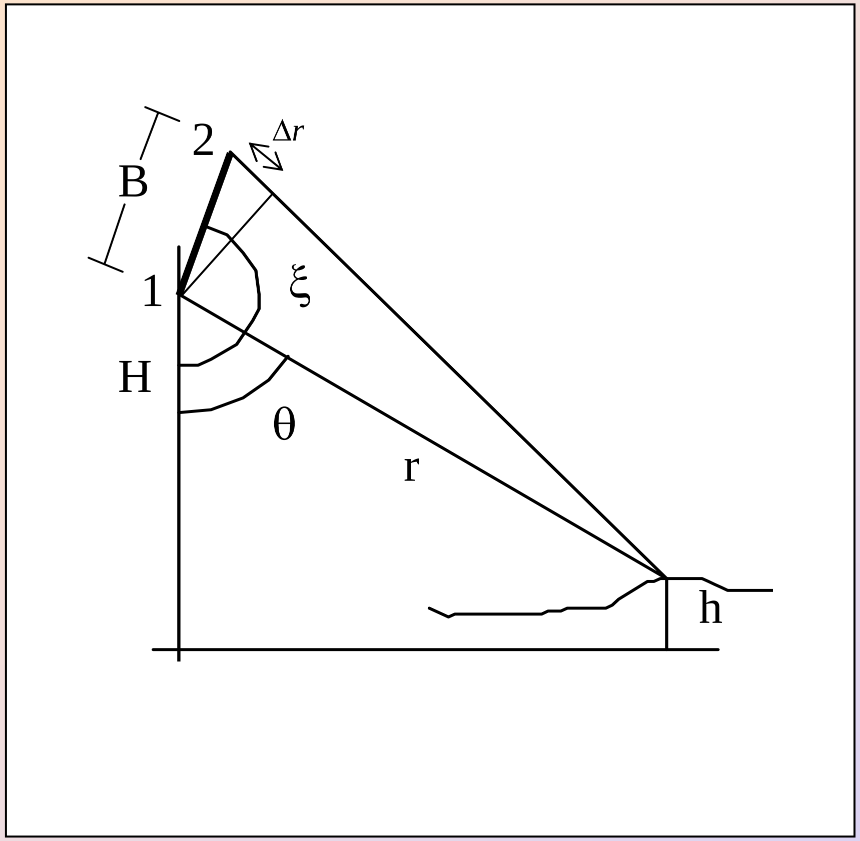

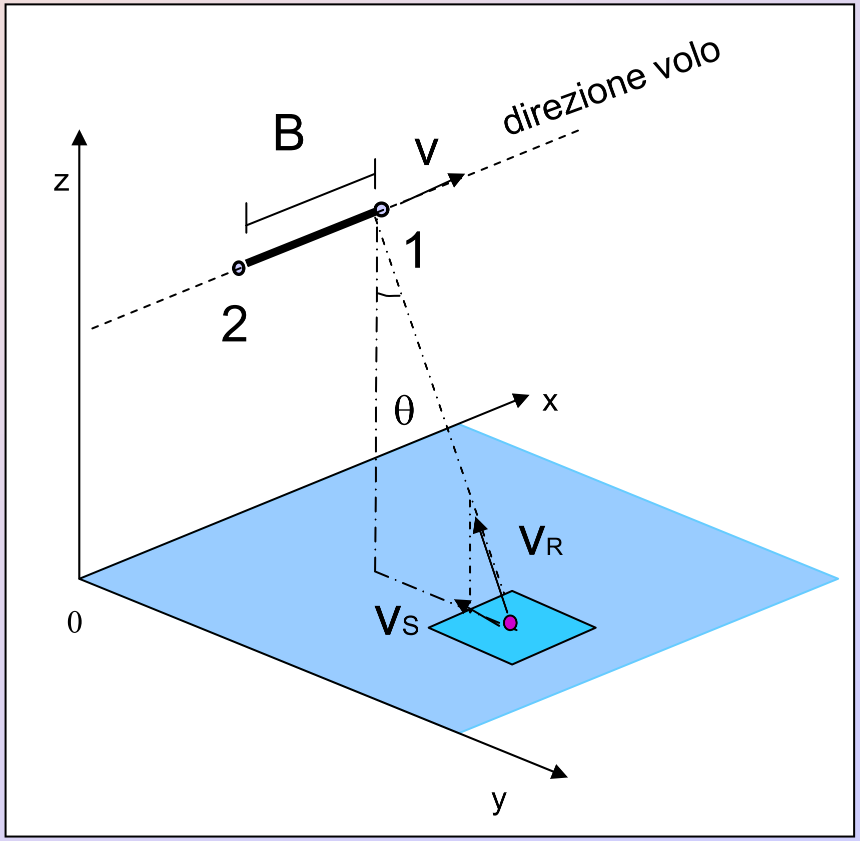

Prodotti principali:

mappe topografiche

mappe correnti marine

Multichannel (MB/MF) InSAR

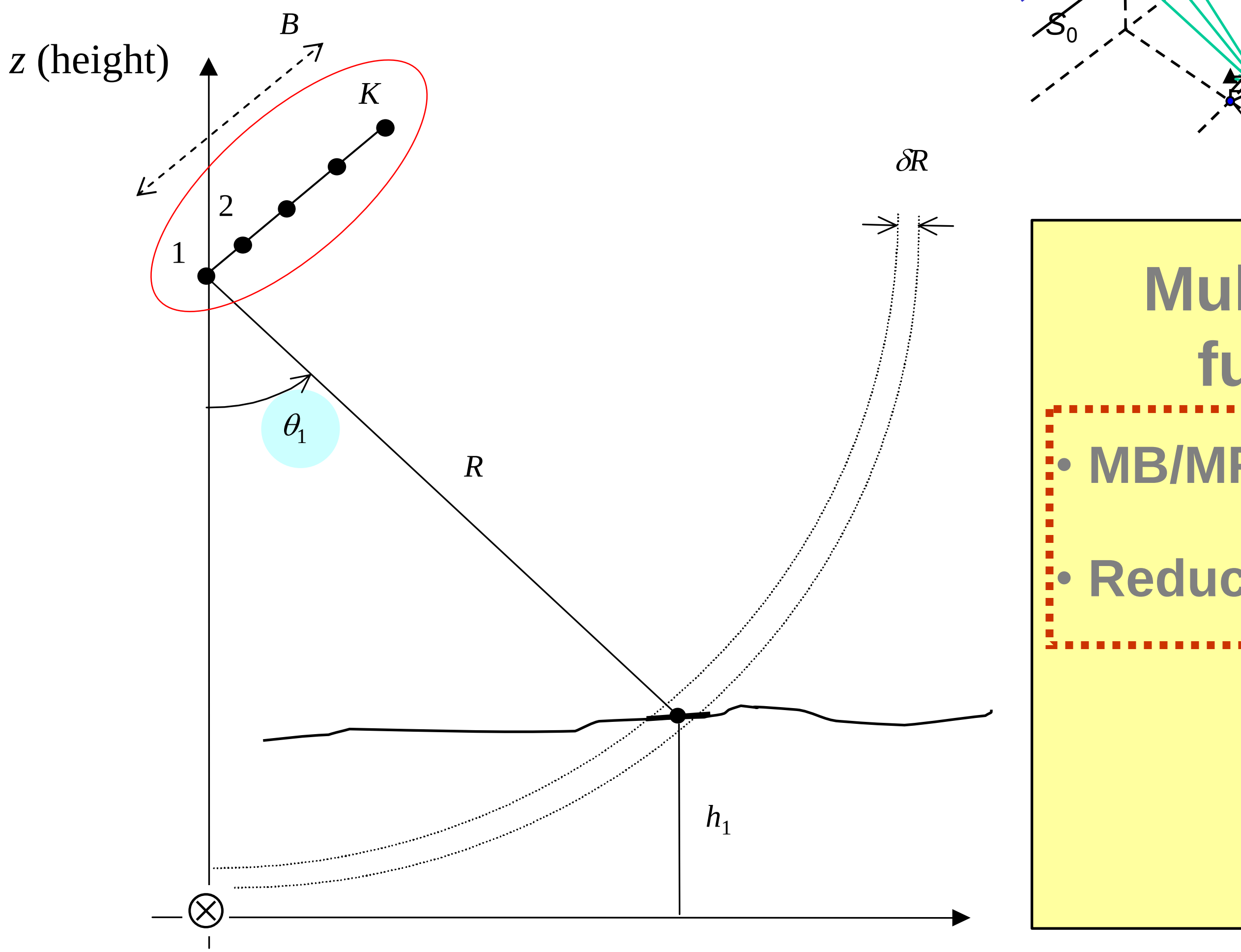

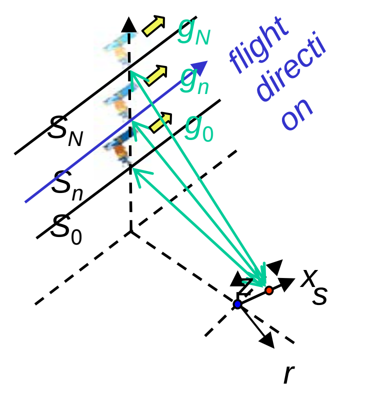

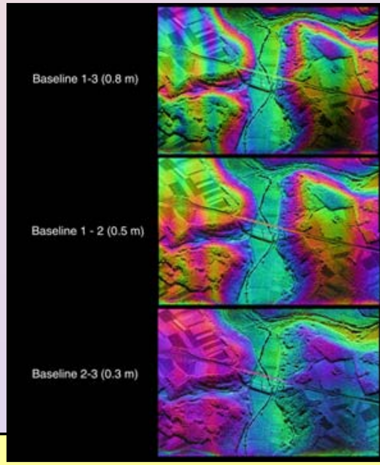

Multich. improved functionalities:

- MB/MF phase unwrapping
- Reduction of data noise

Array processing

$$\mathbf{y}(n) = [y_1(n) \quad y_2(n) \quad \ldots \quad y_K(n)]^T$$

data vector, n=1,2,...N looks

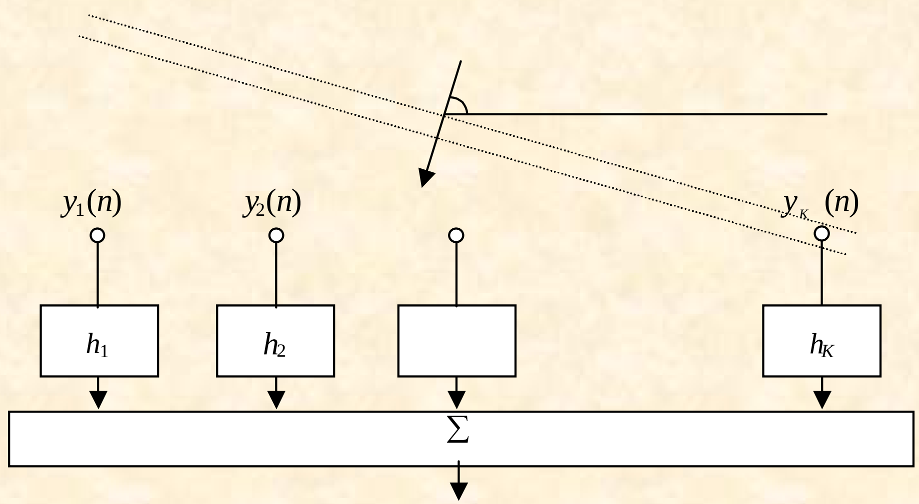

$$y_F(n) = \mathbf{h}^H \mathbf{y}(n)$$

$$\mathbf{a}(\omega) = [1 \quad e^{jl_2\omega} \quad \ldots \quad e^{jl_K\omega}]^T$$

steering vector

Spatial frequency!

FT

$$\hat{P}_B(\omega) = \frac{1}{N}\sum_{i=1}^{N} \Big| \underbrace{\frac{1}{K}\mathbf{a}^H(\omega)}_{\mathbf{h}^H}\mathbf{y}(n) \Big|^2$$

conventional Beamforming

(**multilook Periodogram**)

$$\hat{P}_B(\omega) = \frac{\mathbf{a}^H(\omega)\hat{\mathbf{R}}_y\mathbf{a}(\omega)}{K^2}$$

Multiplicative noise

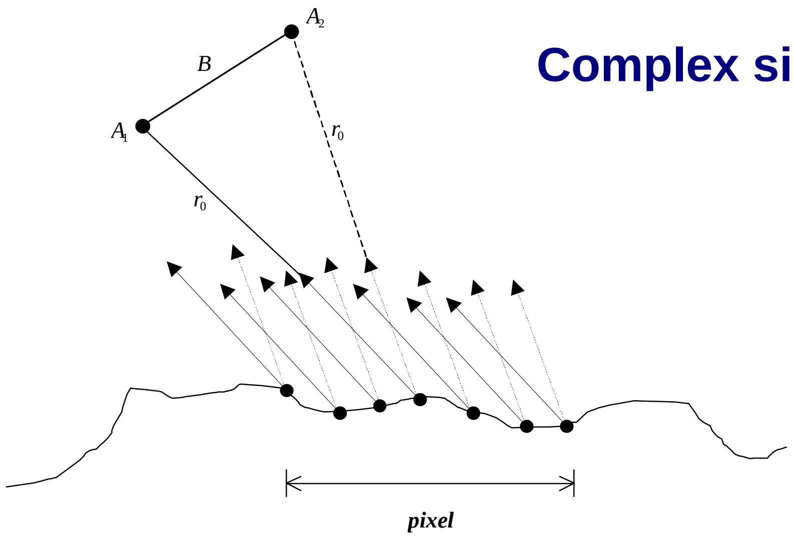

Complex signal (I & Q) at each pixel of the SAR image

Fully developed speckle: complex circular Gaussian distributed

Spatial (baseline) decorrelation: non-line spatial spectrum!

Radar d'immagine (Interferometria, 2.5D)

Frequency MLE
in multiplicative noise

Stima di fase interferometrica (frequenza spaziale)

$$\boxed{\begin{aligned} J(\varphi) = &(\rho_{12} - \rho_{23}\rho_{13})\,\mathrm{Re}\{\exp[-j\varphi(1-p)]\Sigma_{i=1}^{N}\tilde{P}_1^{*(i)}\tilde{P}_2^{(i)}\} + \\ &(\rho_{13} - \rho_{12}\rho_{23})\,\mathrm{Re}\{\exp[-j\varphi]\Sigma_{i=1}^{N}\tilde{P}_1^{*(i)}\tilde{P}_3^{(i)}\} + \\ &(\rho_{23} - \rho_{12}\rho_{13})\,\mathrm{Re}\{\exp[-j\varphi p]\Sigma_{i=1}^{N}\tilde{P}_2^{*(i)}\tilde{P}_3^{(i)}\} \end{aligned}}$$

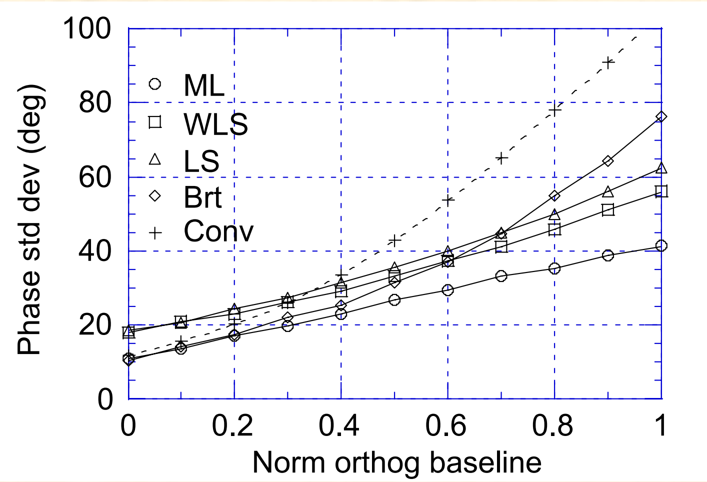

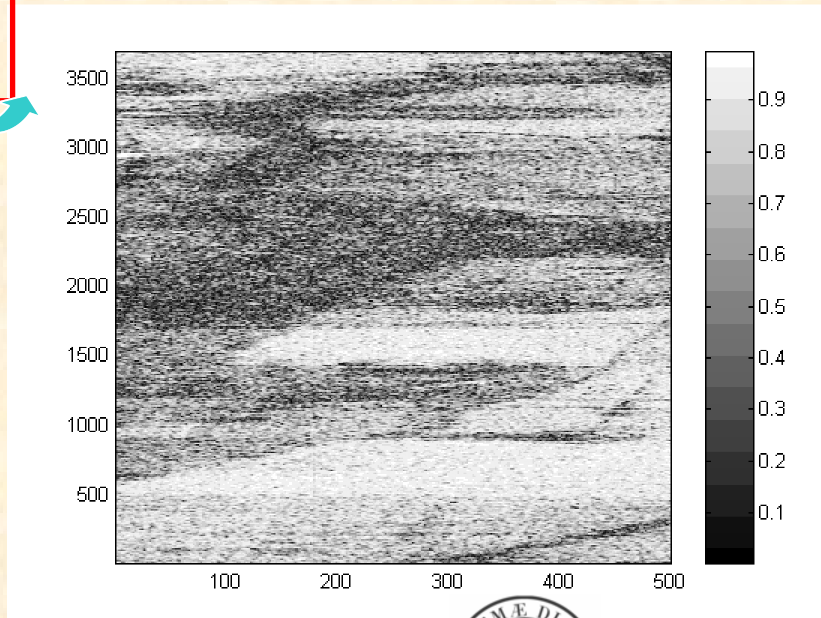

Multibaseline (MB) InSAR

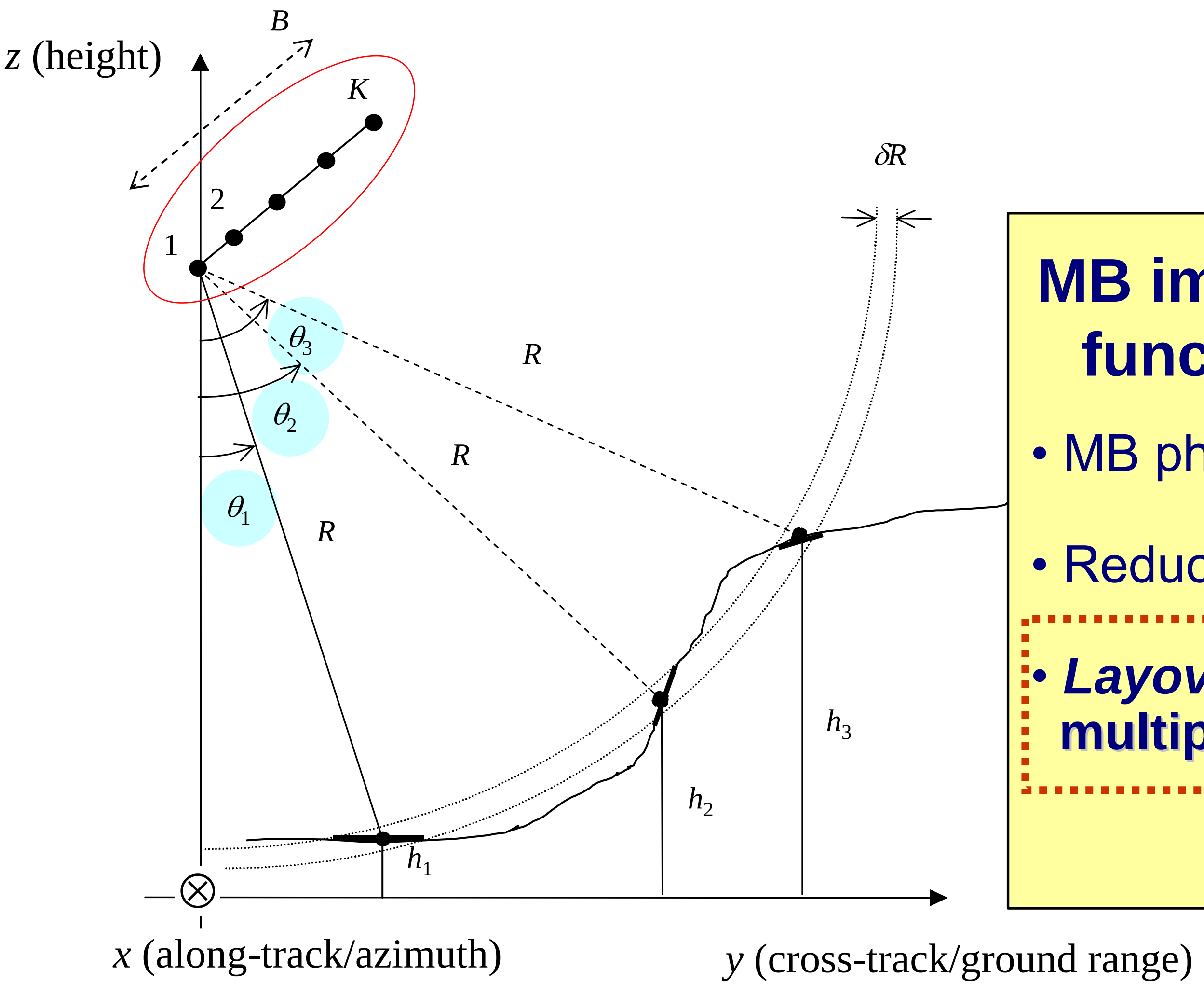

MB improved/new functionalities:

- MB phase unwrapping
- Reduction of data noise
- ***Layover*** **overcoming: multiple DOAs estimation**

Superresolution

Zero spatial bandwidth

$$K = 3,\ N_s = 2 \qquad \sigma_v^2 = 0: \quad \mathbf{y}(n) = \alpha_1(n)\mathbf{a}(\varphi_1) + \alpha_2(n)\mathbf{a}(\varphi_2) = \begin{bmatrix} | & | \\ \mathbf{a}_1 & \mathbf{a}_2 \\ | & | \end{bmatrix} \begin{bmatrix} \alpha_1 \\ \alpha_2 \end{bmatrix}$$

Array manifold

Signal subspace $\rightarrow N_s, \{\varphi_m\}$

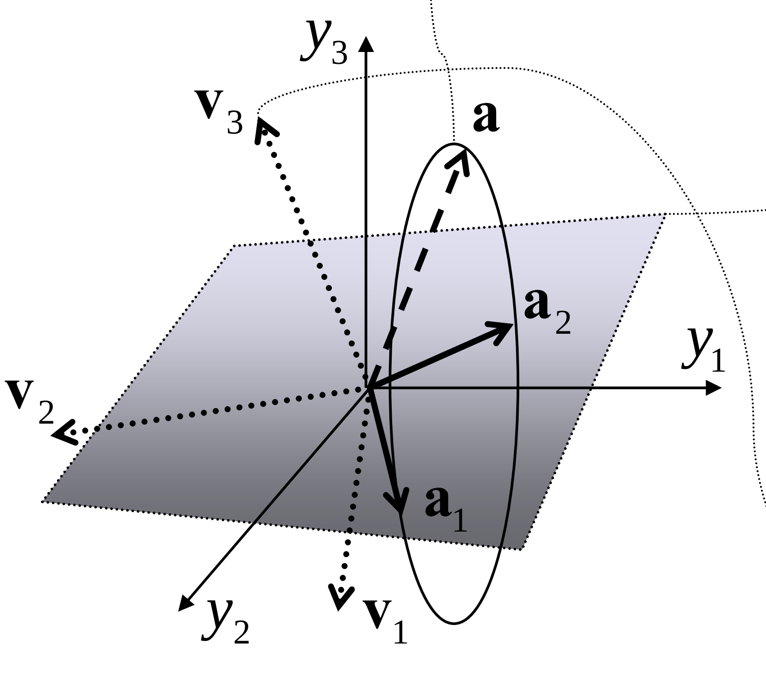

$$\mathbf{C}_\mathbf{y} = \begin{bmatrix} | & | \\ \mathbf{a}_1 & \mathbf{a}_2 \\ | & | \end{bmatrix} \begin{bmatrix} \tau_1 & \\ & \tau_2 \end{bmatrix} \begin{bmatrix} - & \mathbf{a}_1^H & - \\ - & \mathbf{a}_2^H & - \end{bmatrix}$$

$$\mathit{Range}[\mathbf{C}_\mathbf{y}] = \mathit{Signal\ subspace}$$

Parametric spectral estimation

“Noise” subspace

Airborne experimental results: FGAN-FHR AER-II

Center frequency	10.0 GHz
Resolution	1 m
Range	20 km
XTI channels	3 parallel receive channels, overall baseline 0.8 m
Antenna	Active phased array, 16 T/R modules + auxiliary antennas
Transmit power	80 W
Polarisation	VV (HH / HV / VH)

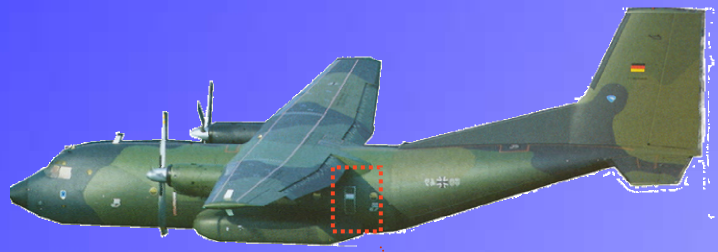

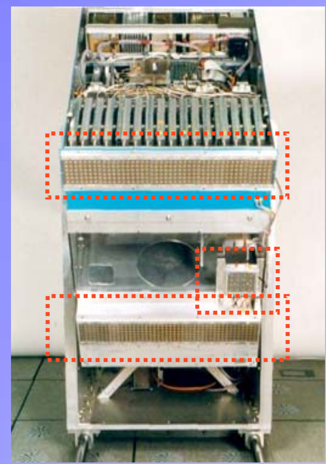

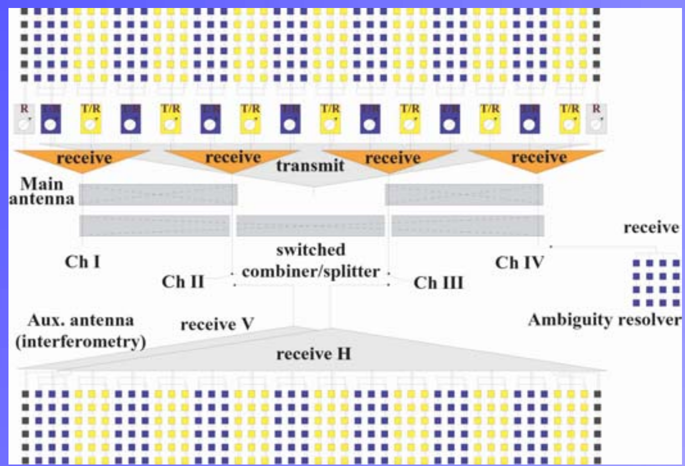

Airborne multiantenna results (FGAN AER-II)

Neckar river valley and highway bridge, Weitingen, Germany

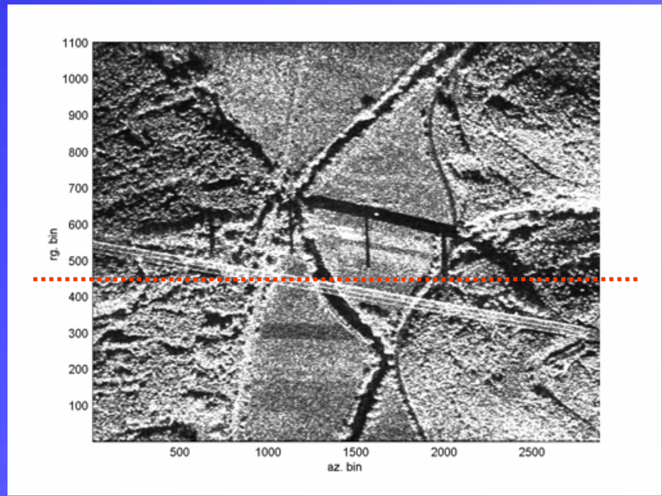

- THERMAL NOISE EQUALIZATION
- PHASE CALIBRATION
- AMPLITUDE CALIBRATION
- DERAMPING AND ORTHO BASELINE EVALUATION

Height resolution 98 m

Ambiguous height 370 m

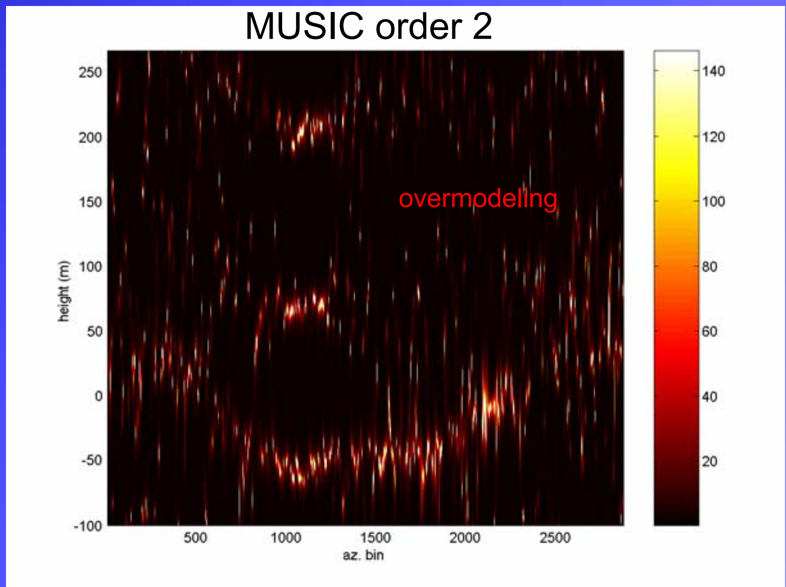

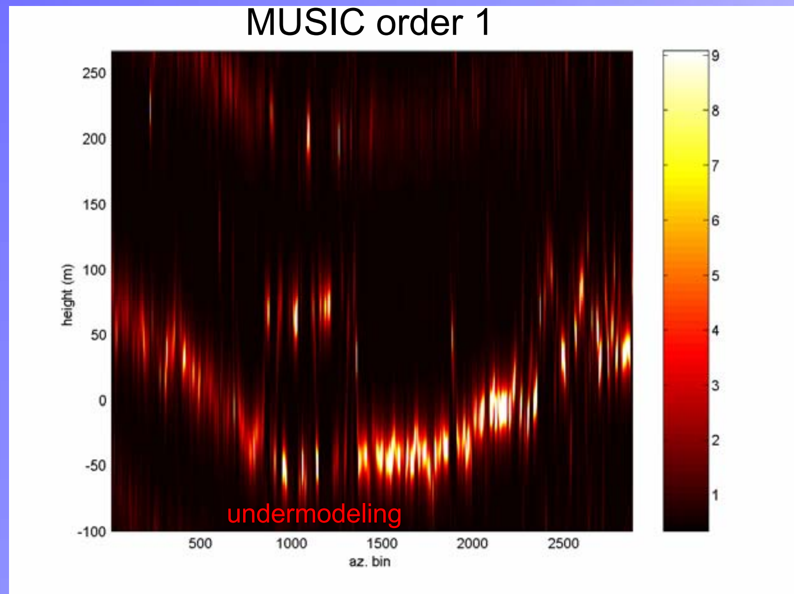

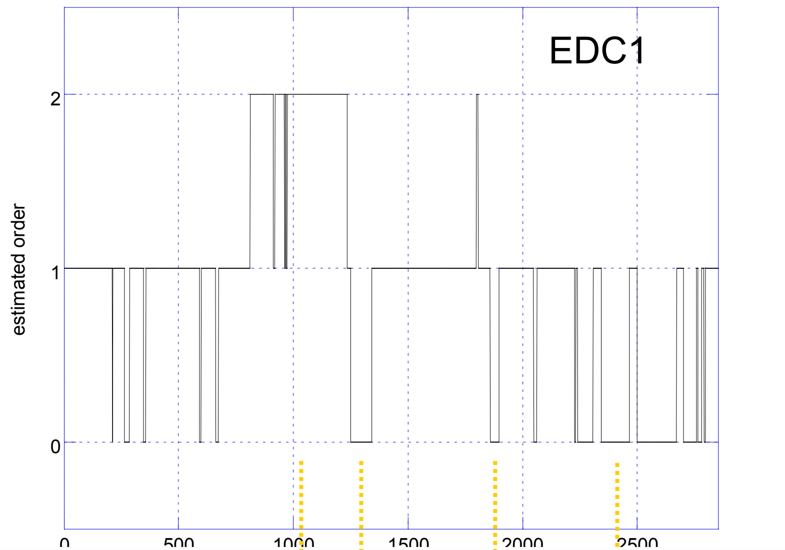

Numero di look pari a 33 looks, stabilizzazione degli autovalori

Prestazione della stima dell'ordine: 90%

r, g, b: $\hat{N}_s = 2, 1, 0$

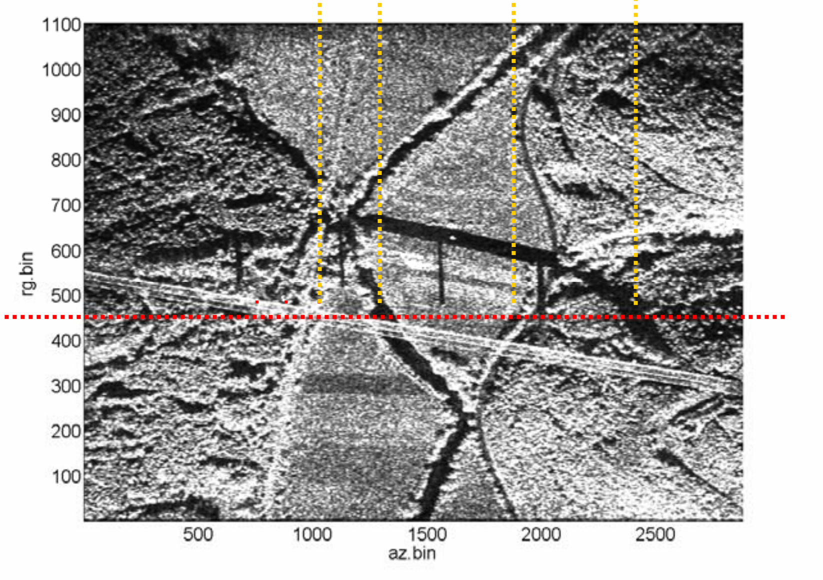

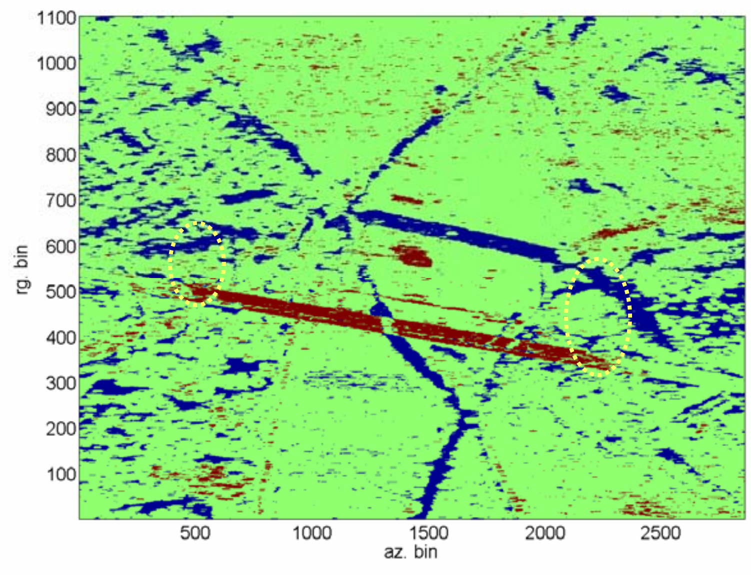

Metodo integrato

EDC-MUSIC

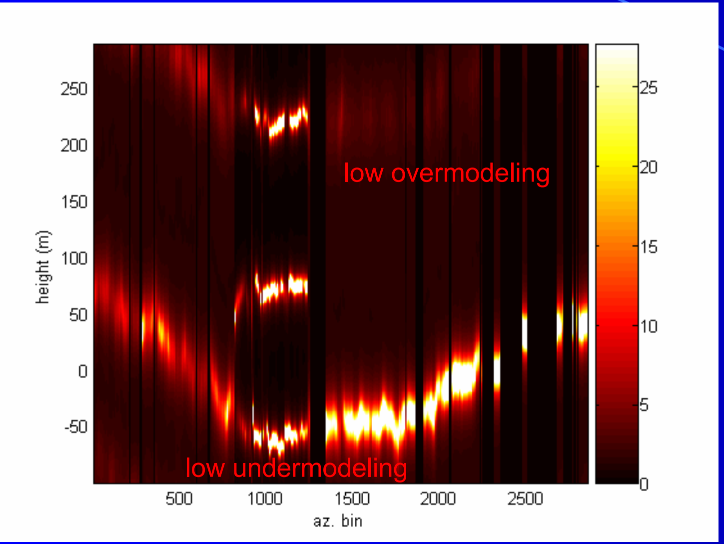

EDC-MUSIC

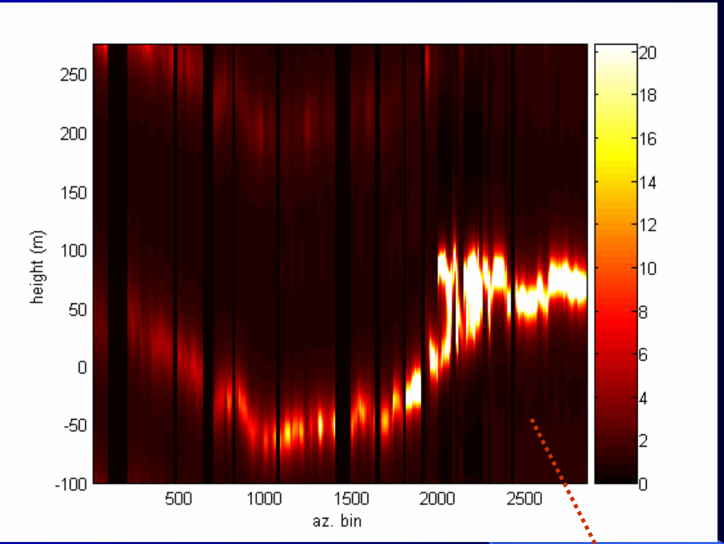

Post-processing: si sfruttano le info a priori sul settore in quota in cui sono contenuti I picchi da MUSIC

Altezze in layover estratte

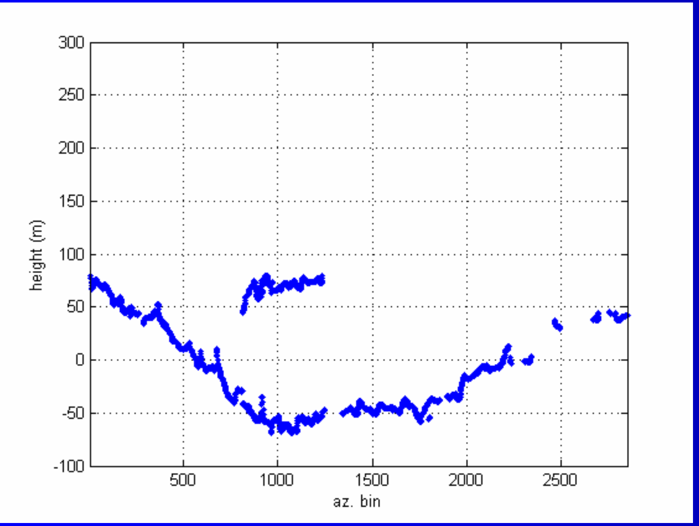

Altezze in layover estratte

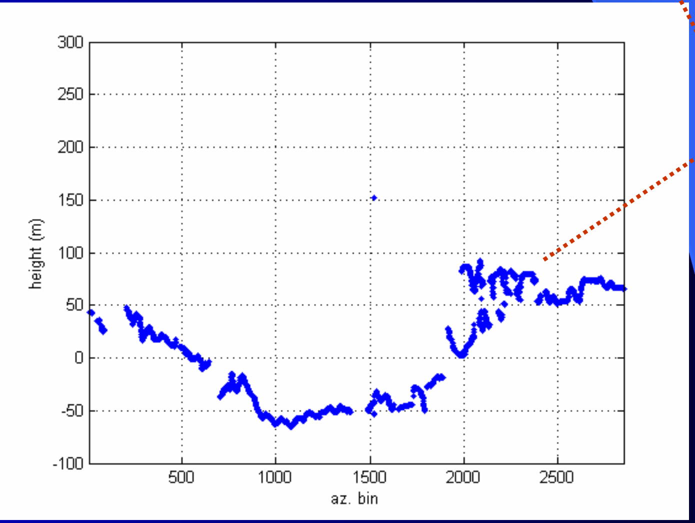

bridge
end

Urban DEM layover problem

Complex structures/discontinuous surfaces → **layover** → multicomponent signal

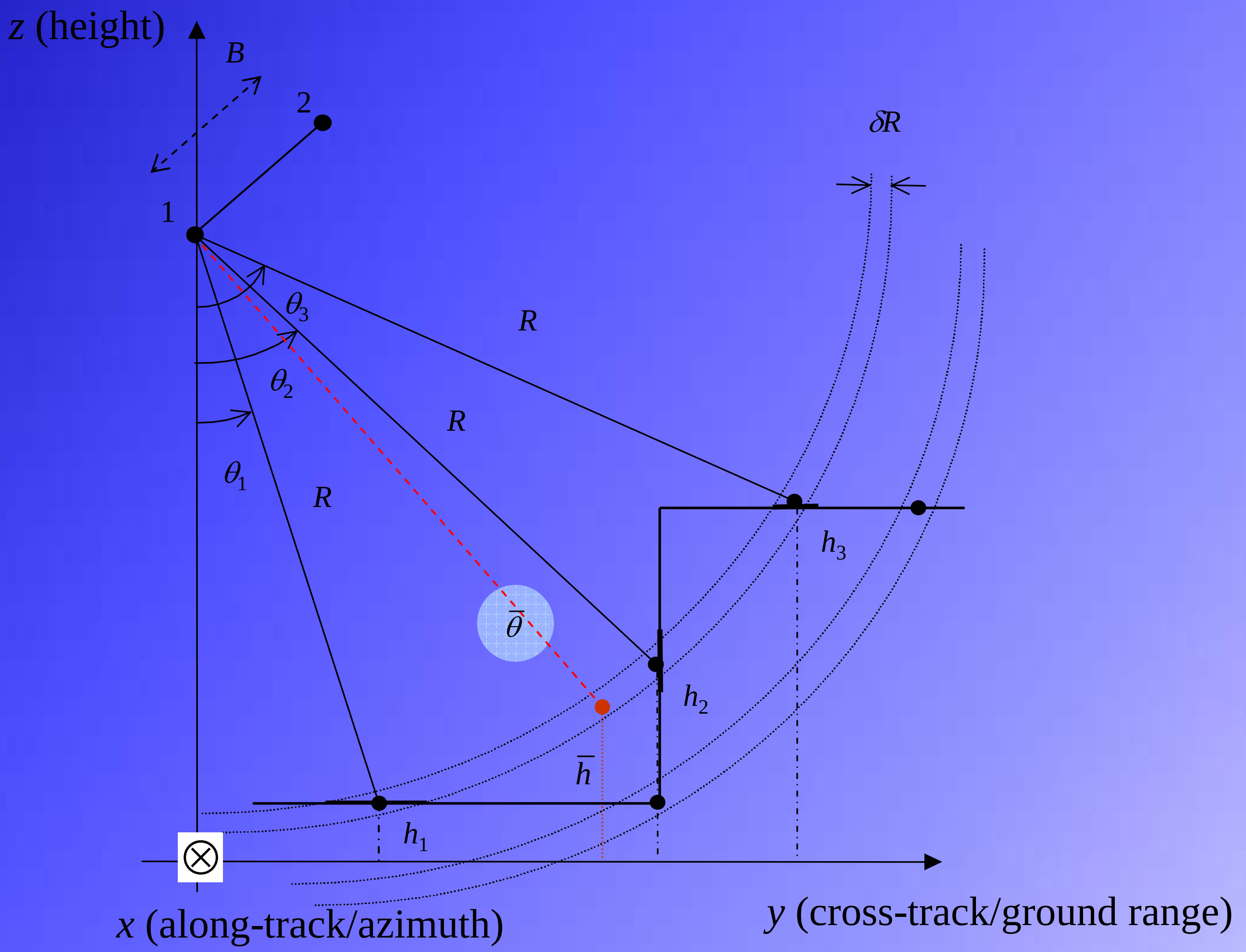

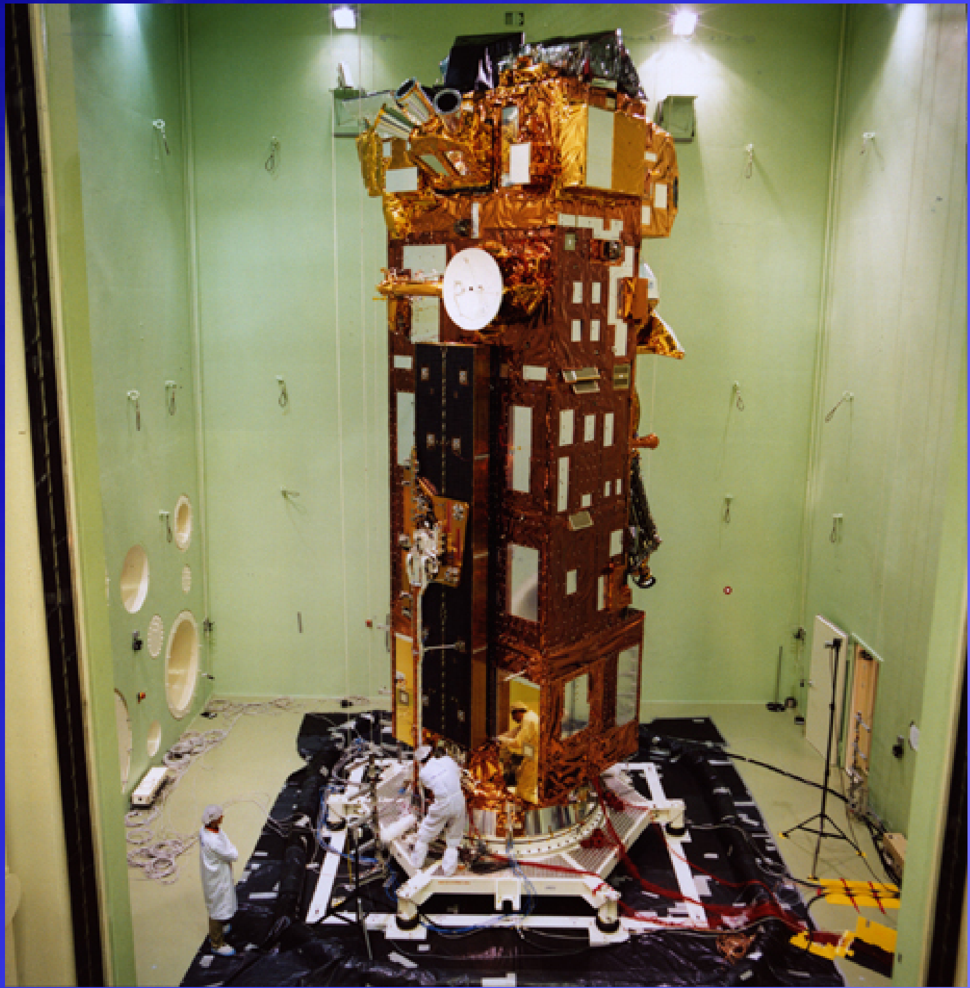

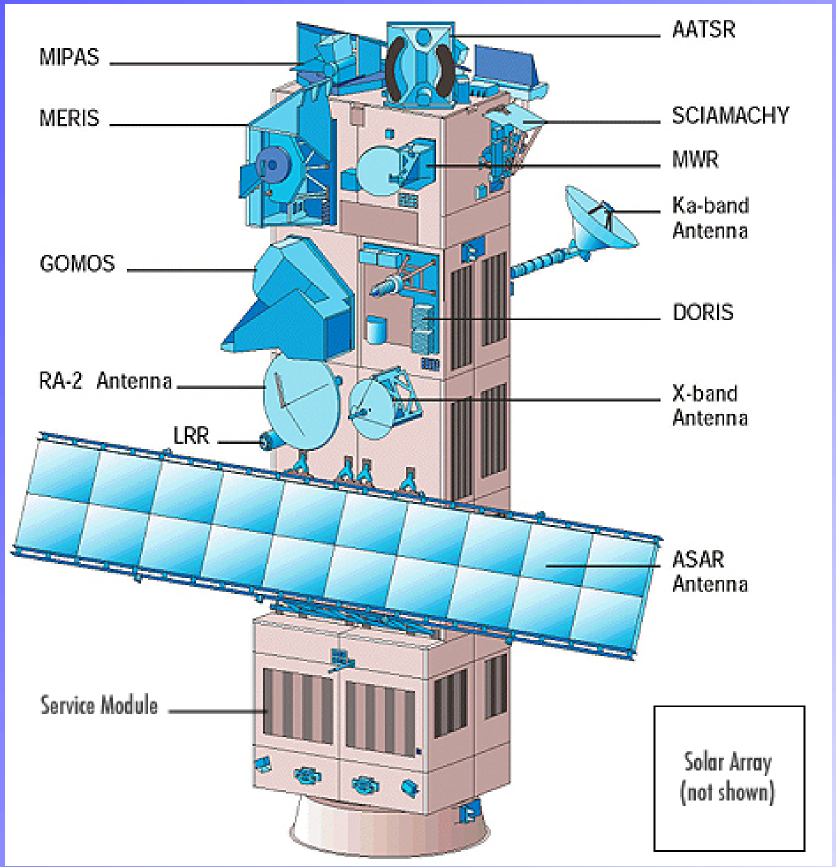

MIPAS
MERIS
GOMOS
RA-2 Antenna
LRR
AATSR
SCIAMACHY
MWR
Ka-band Antenna
DORIS
X-band Antenna
ASAR Antenna
Service Module
Solar Array (not shown)

S.Paolo Stadium

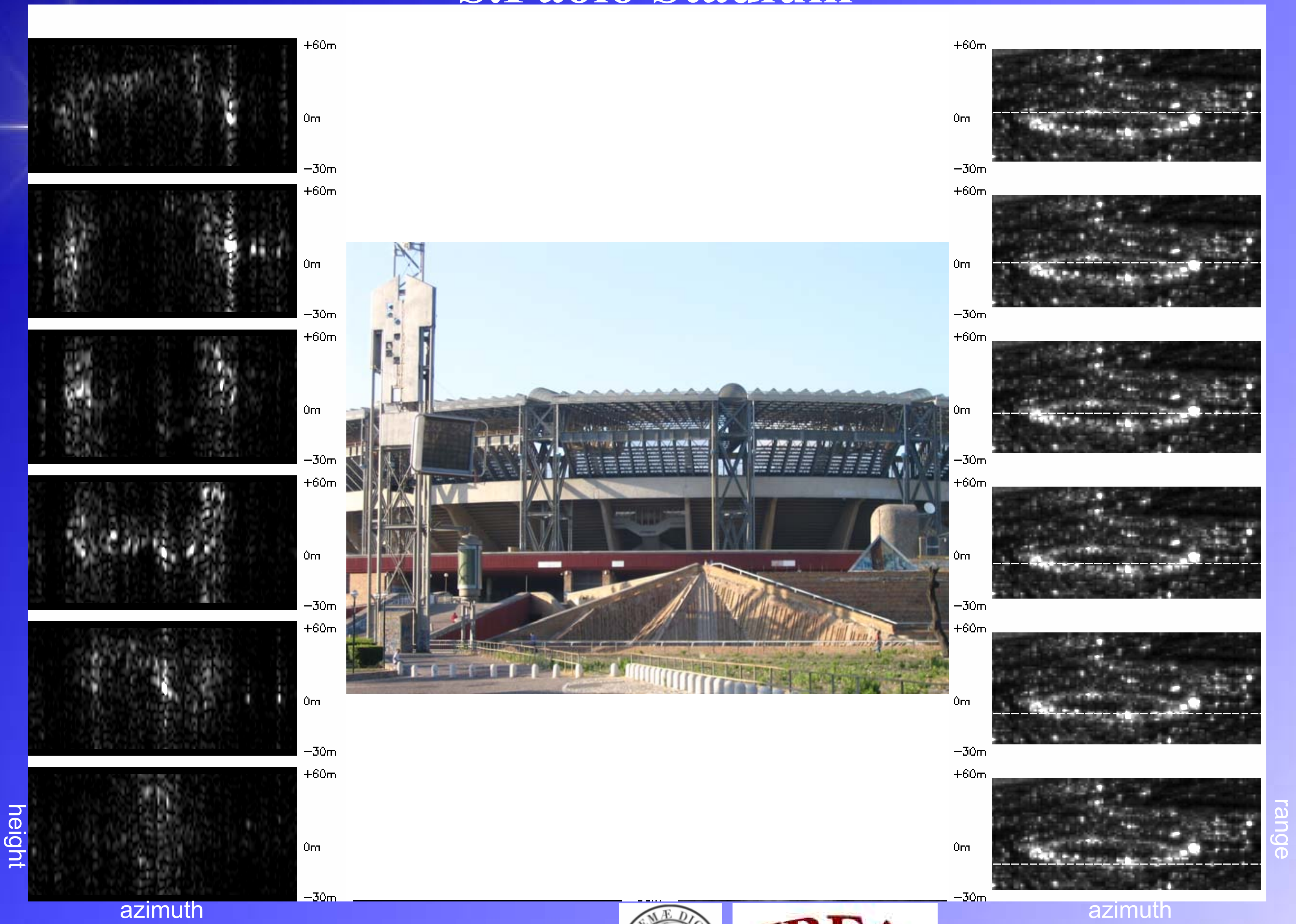

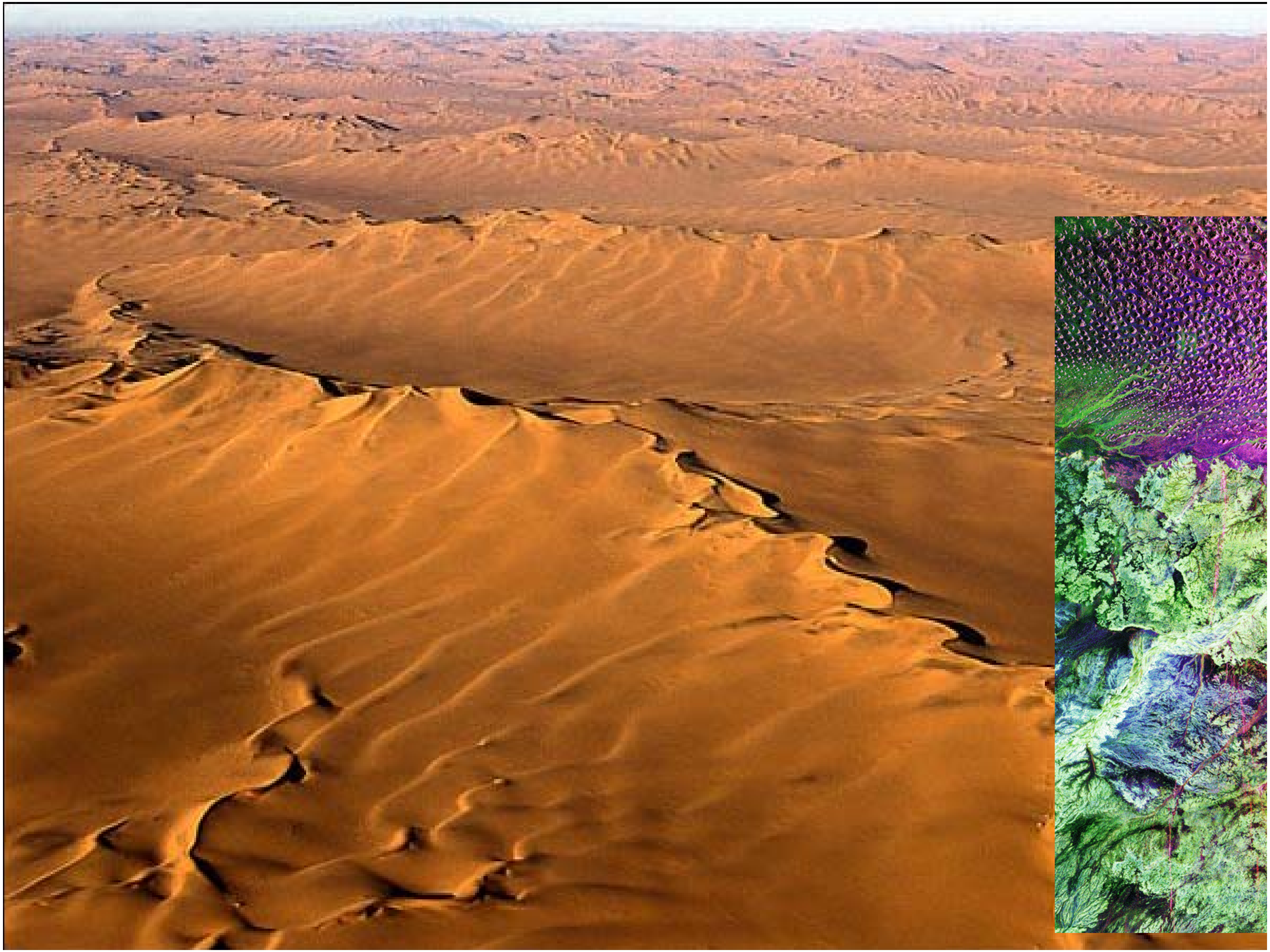

Radar Tomography: full 3-D

Layover: the illuminated 3-D reflectivity **a(x,y,z)** has been assumed to be concentrated to a 2-D surface

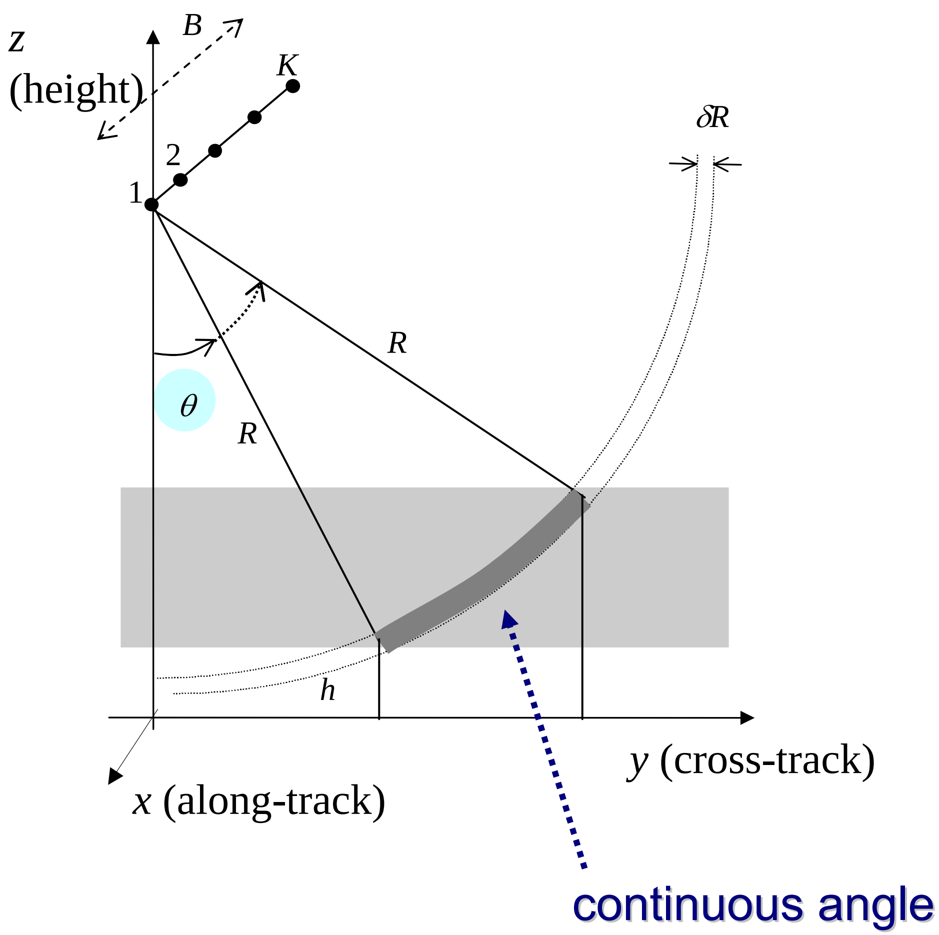

Aim of XTI-SAR:

extract τ_i and θ_i from data

from 2.5-D to 3-D

SAR-Tomography (full 3-D):

when **a(θ)** is continuous w.r.t. θ, not discrete

"TAC" radar!

Radar d'immagine (Tomografici, Full 3D)

E-SAR **DLR**
L-band, VV

DGPS+INS

K=14 tracks
overall baseline: L=240 m

site: **Oberpfaffenhofen Germany**

Fourier height resolution: 3 m
unambiguous height range: 35 m

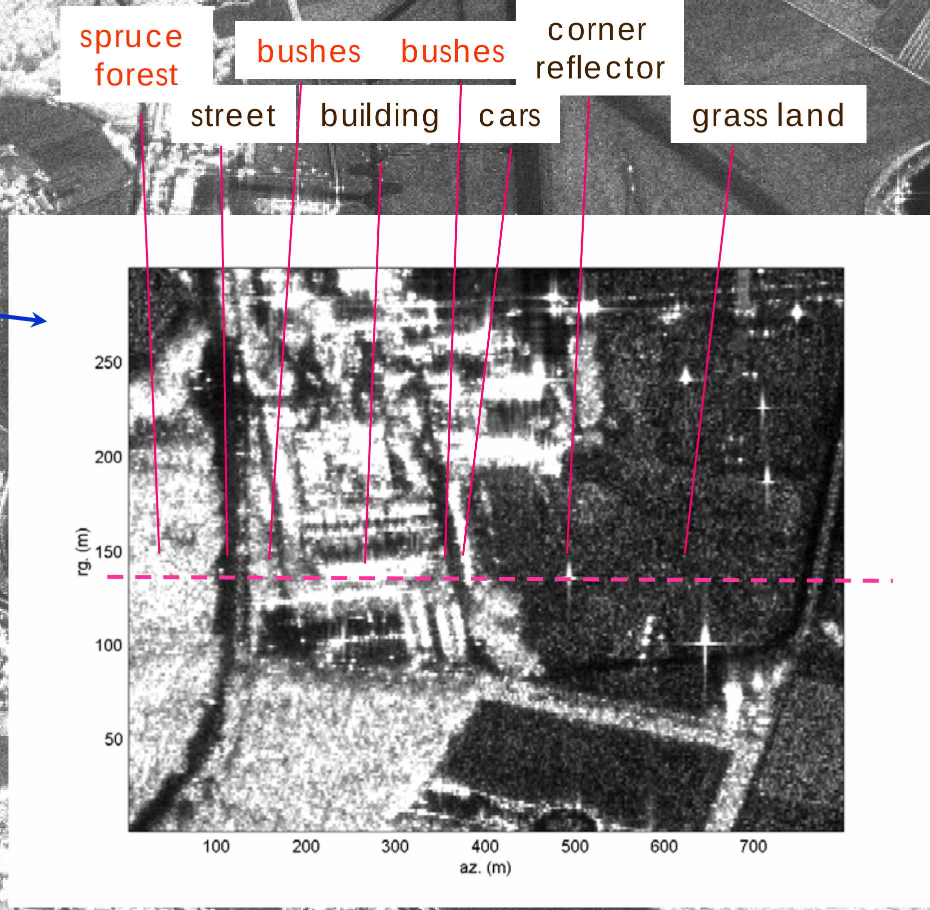

MB phase calibration:
corner reflector

Radar d’immagine (Tomografici, Full 3D)

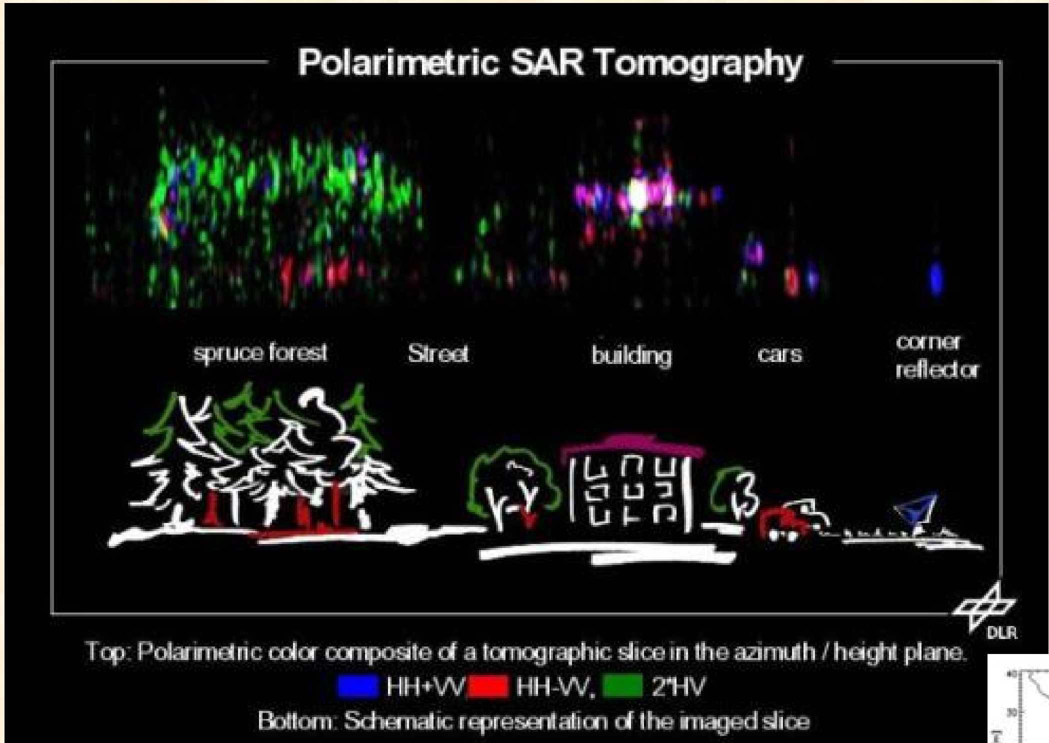

Stima spettrale spaziale
non-parametrica

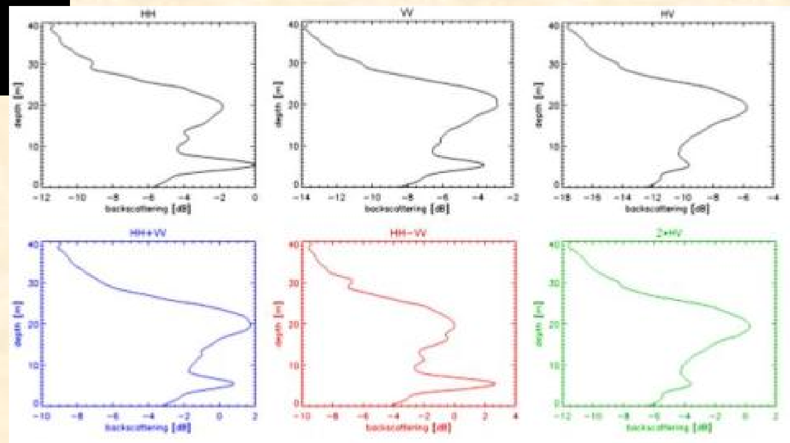

Current Problems of Radar Tomography

Wide field of potential applications, but:

Tradeoff ambiguity distance/z-resolution for given number K of tracks

Limited z-resolution, many tracks required

Typically irregular track distribution:

Anomalous sidelobes in the PSF !
(quasi-grating lobes)

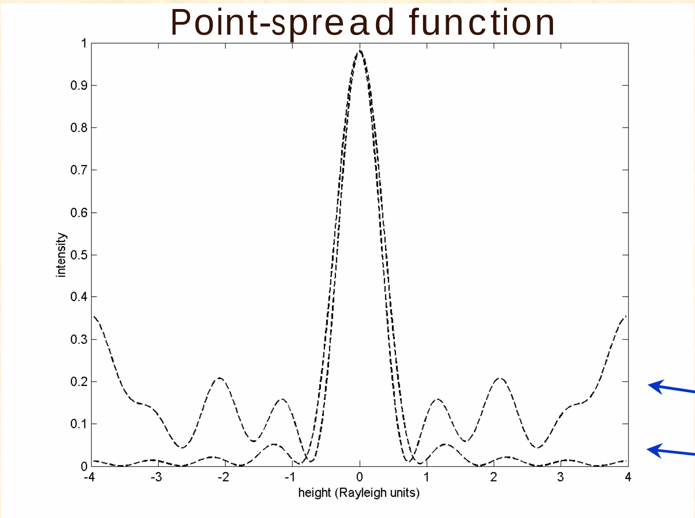

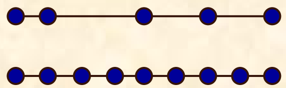

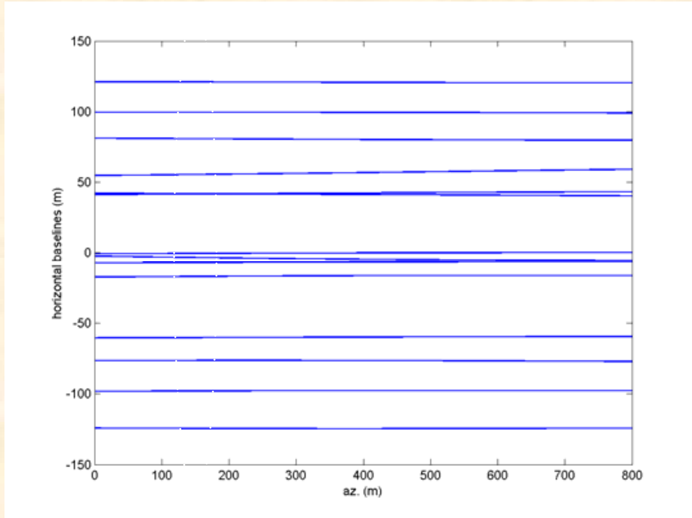

E-SAR, DLR

Stima spettrale non-parametrica *adattiva*

Lobi laterali $\rightarrow$ leakage $\rightarrow$ masking

Stima spettrale non-parametrica *adattiva*

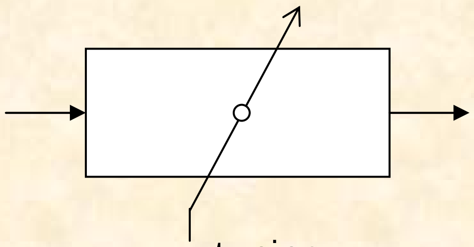

tuning

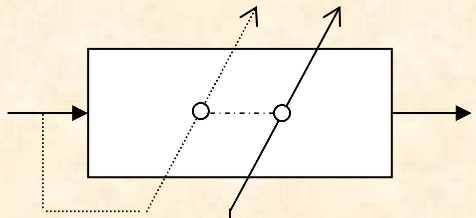

data-dependent
interference rejection

tuning

leakage suppression

Il filtro di Capon

Stima MVU
Filtro sbiancante ad. + Period.

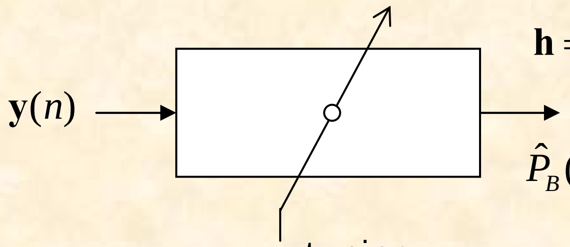

tuning

$$\mathbf{h} = \frac{\mathbf{a}(\omega)}{K}$$

$$\hat{P}_B(\omega) = \frac{\mathbf{a}^H(\omega)\hat{\mathbf{R}}_y\mathbf{a}(\omega)}{K^2}$$

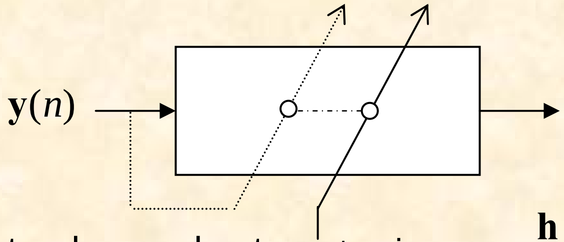

data-dependent
interference rejection

tuning

$$\mathbf{h} = \frac{\mathbf{R}_y^{-1}\mathbf{a}(\omega)}{\mathbf{a}^H(\omega)\mathbf{R}_y^{-1}\mathbf{a}(\omega)}$$

$$\hat{P}_C(\omega) = \frac{1}{\mathbf{a}^H(\omega)\hat{\mathbf{R}}_y^{-1}\mathbf{a}(\omega)}$$

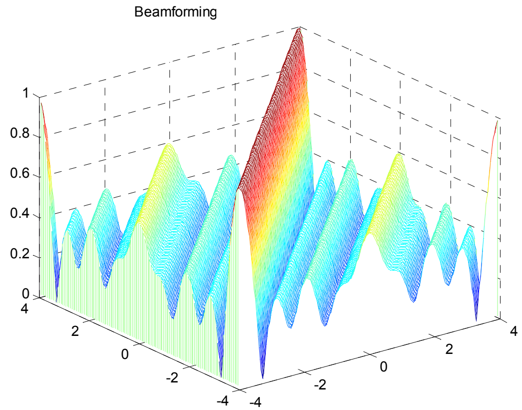

frequency response

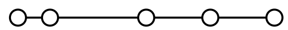

N=32 looks   SNR=9, 12 dB

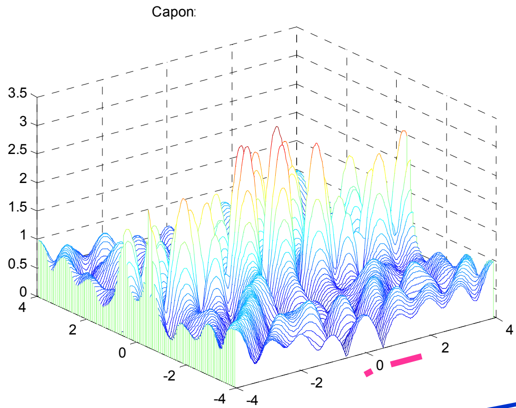

reduced leakage by adaptivelysetting nulls !

simulated comparison

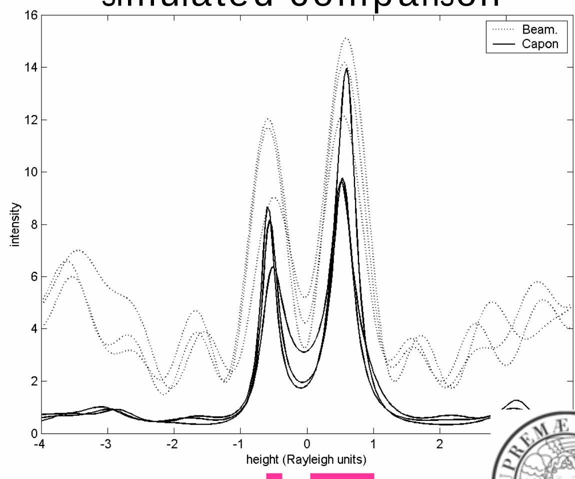

Radar d’immagine (Tomografici, Full 3D)

spatial Periodogram

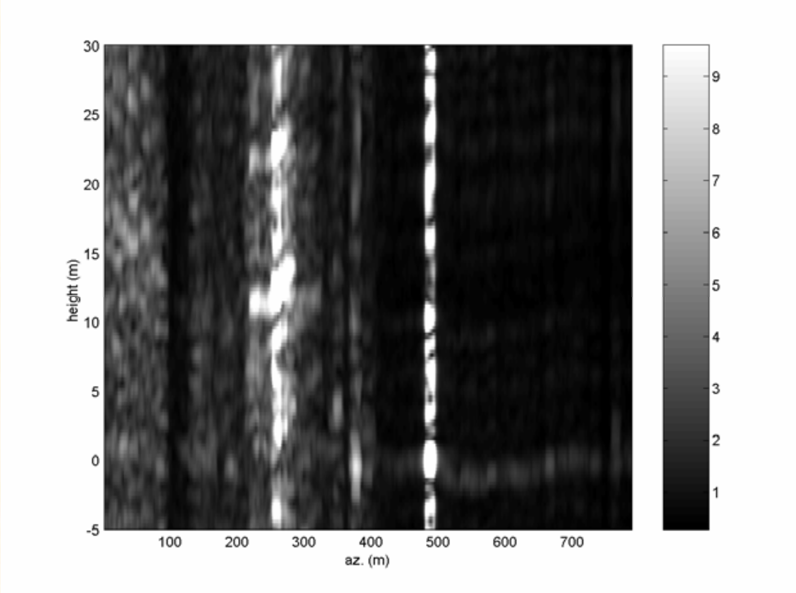

Capon

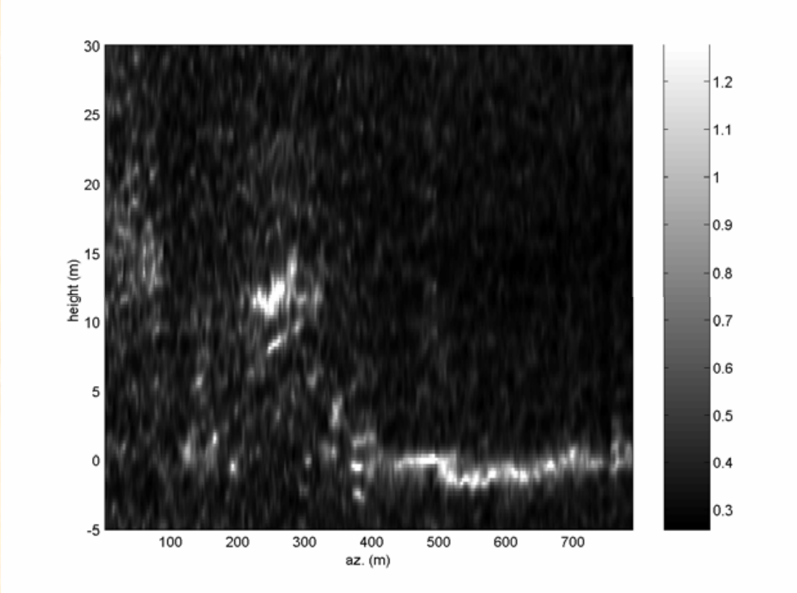

amplitude,
arbitrary units

amplitude,
arbitrary units

K=14 tracks

N=13 obs.

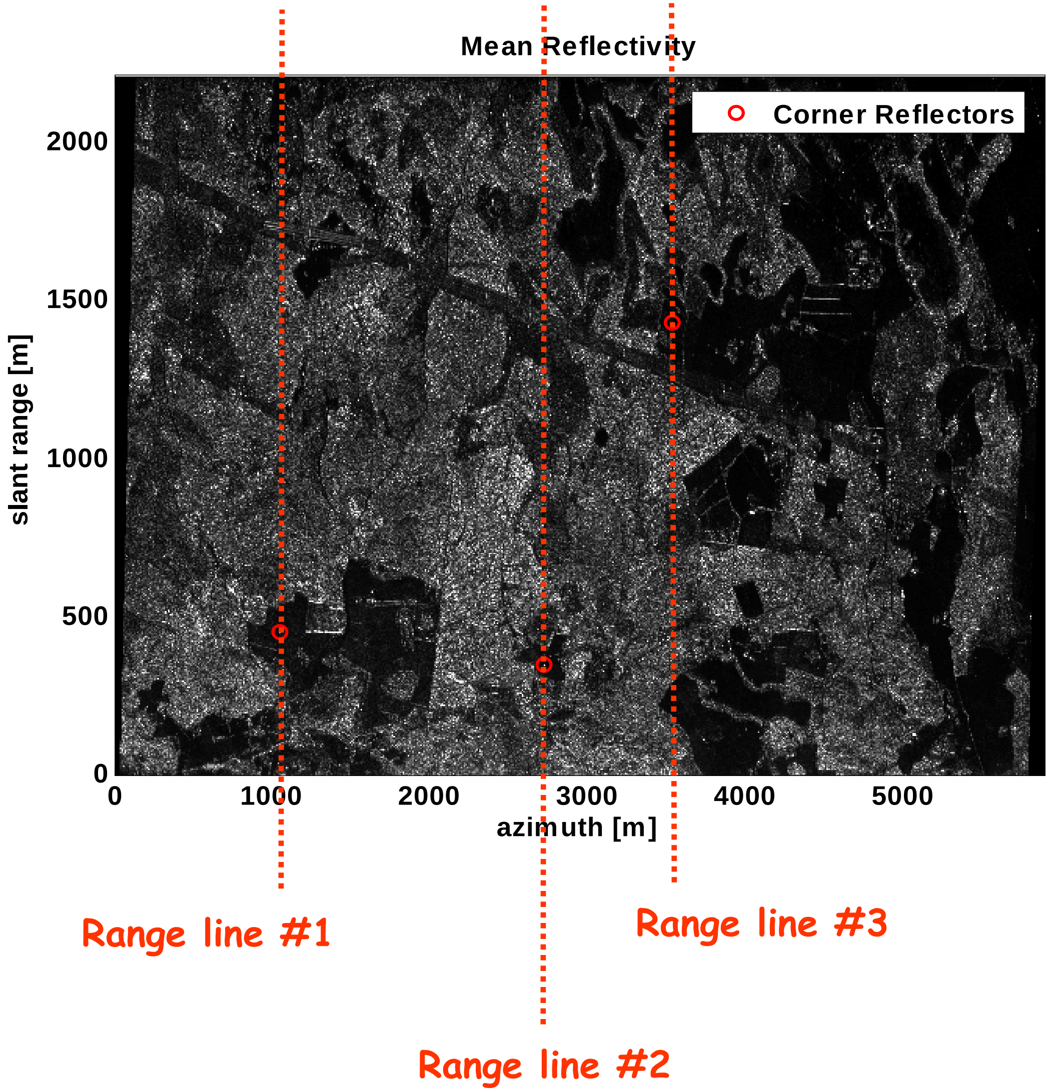

Mean Reflectivity
Corner Reflectors
slant range [m]
azimuth [m]
2000
1500
1000
500
0
0
1000
2000
3000
4000
5000
Range line #1
Range line #2
Range line #3

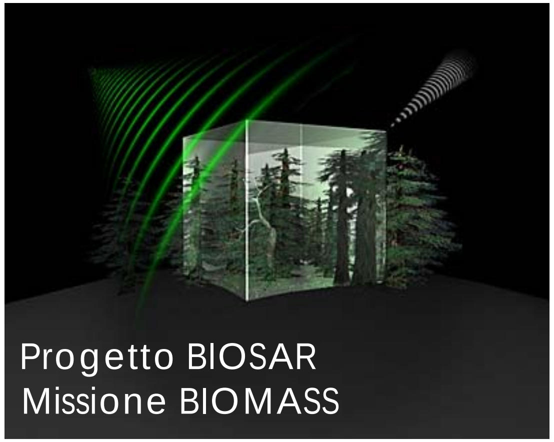

Progetto BIOSAR
Missione BIOMASS

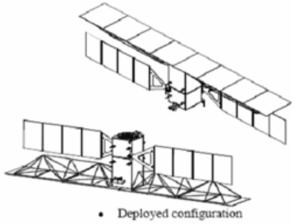

• Deployed configuration

P-band data analysis

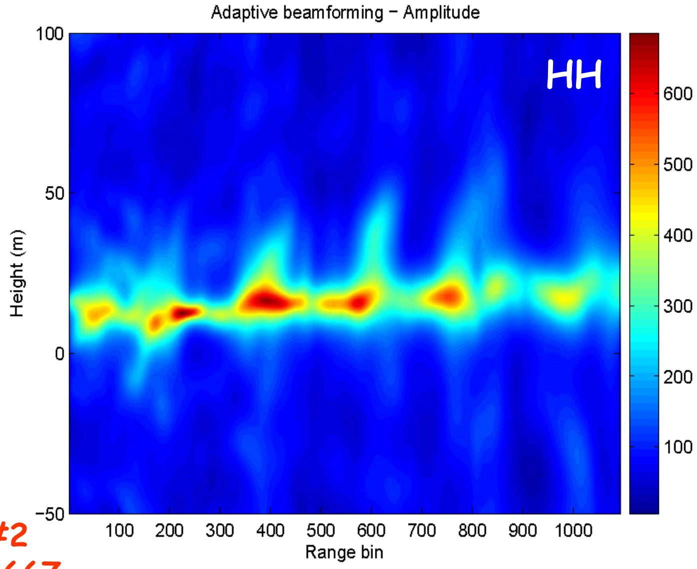

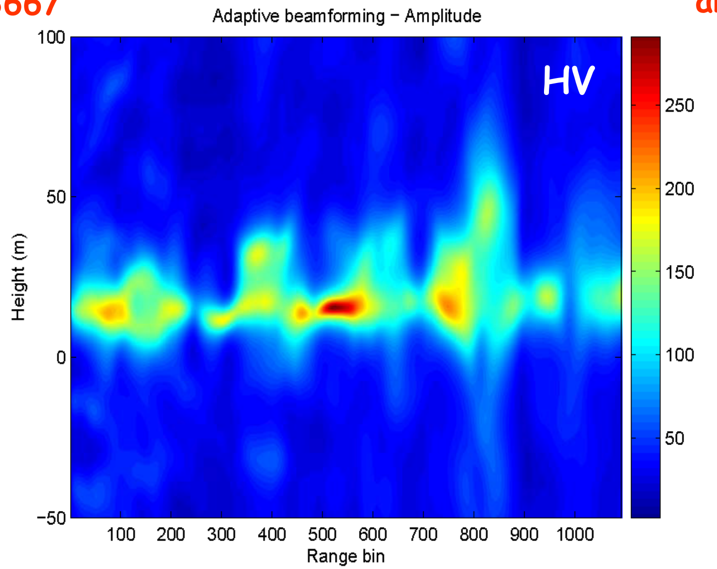

Range line #2
abs. az. bin 3667
(Capon)

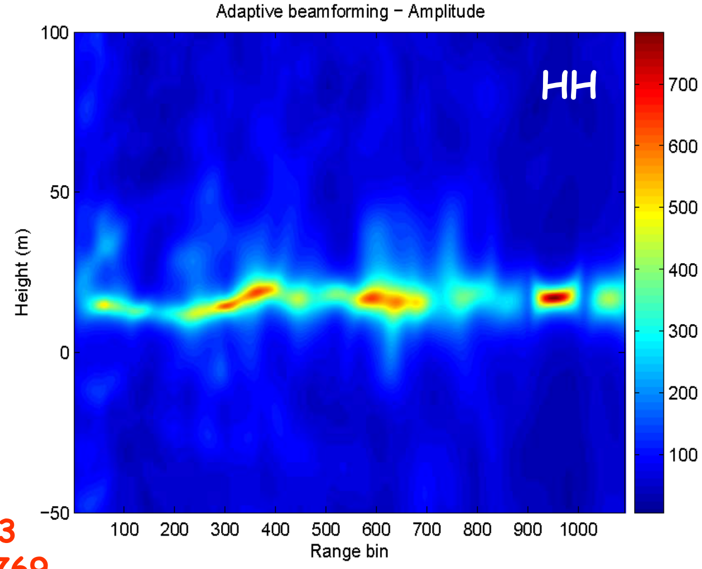

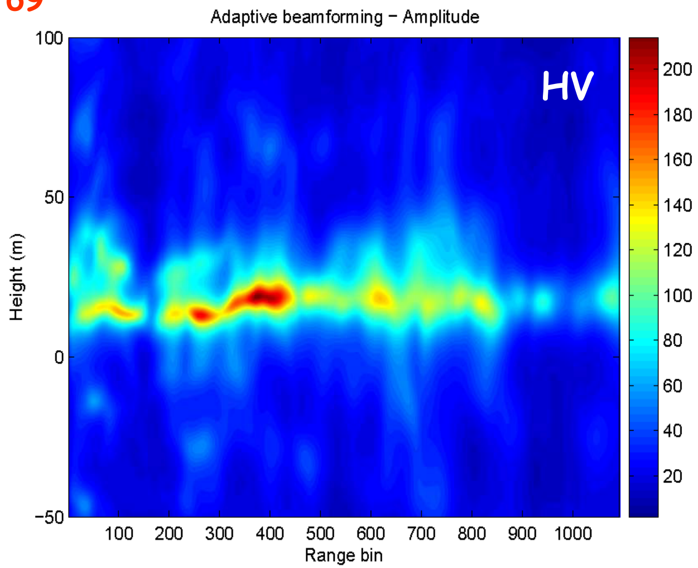

Range line #3
abs. az. bin 4769
(Capon)

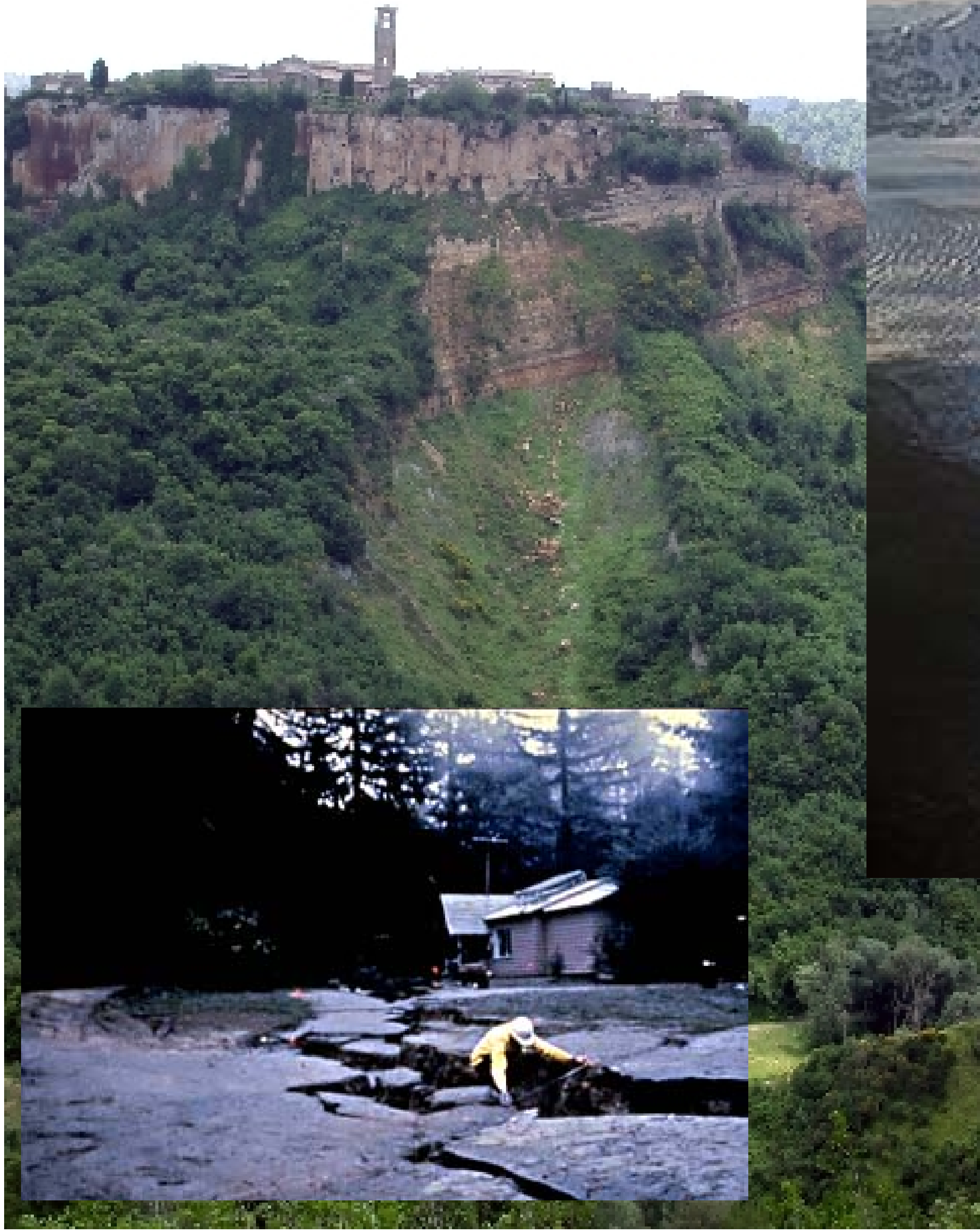

Differential Imaging

3D Tomo-SAR: multi-baseline

→ layover solution, h-backscatter profiling; recently introduced

D-InSAR: multiple-pass

→ *displacements (single h-estimation); operational technique*

"micro-Doppler" technique
(phase time changes: ***temporal* frequency**)

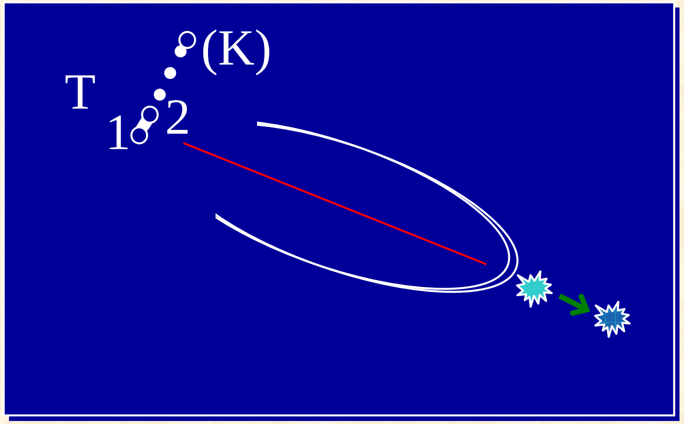

Beamforming technique
(***spatial* frequencies**)

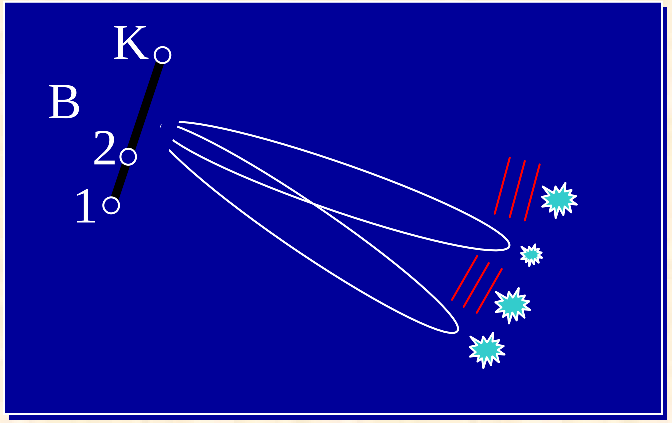

Radar d'immagine

(Tecniche Differenziali)

Applicazioni: analisi subsidenze, fronti di frana, faglie, terremoti, …

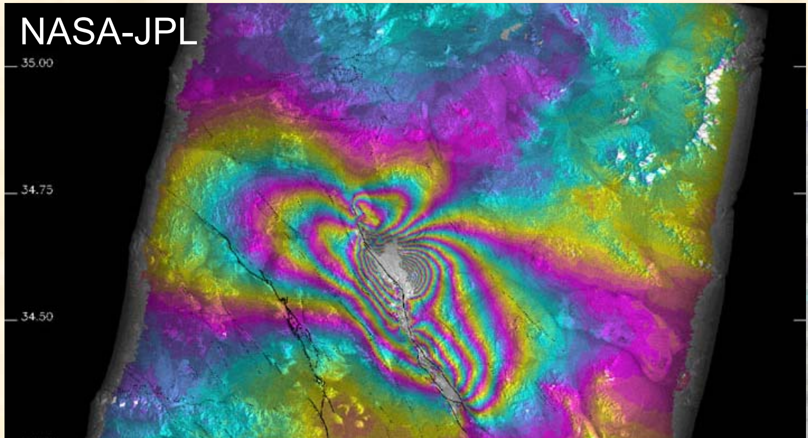

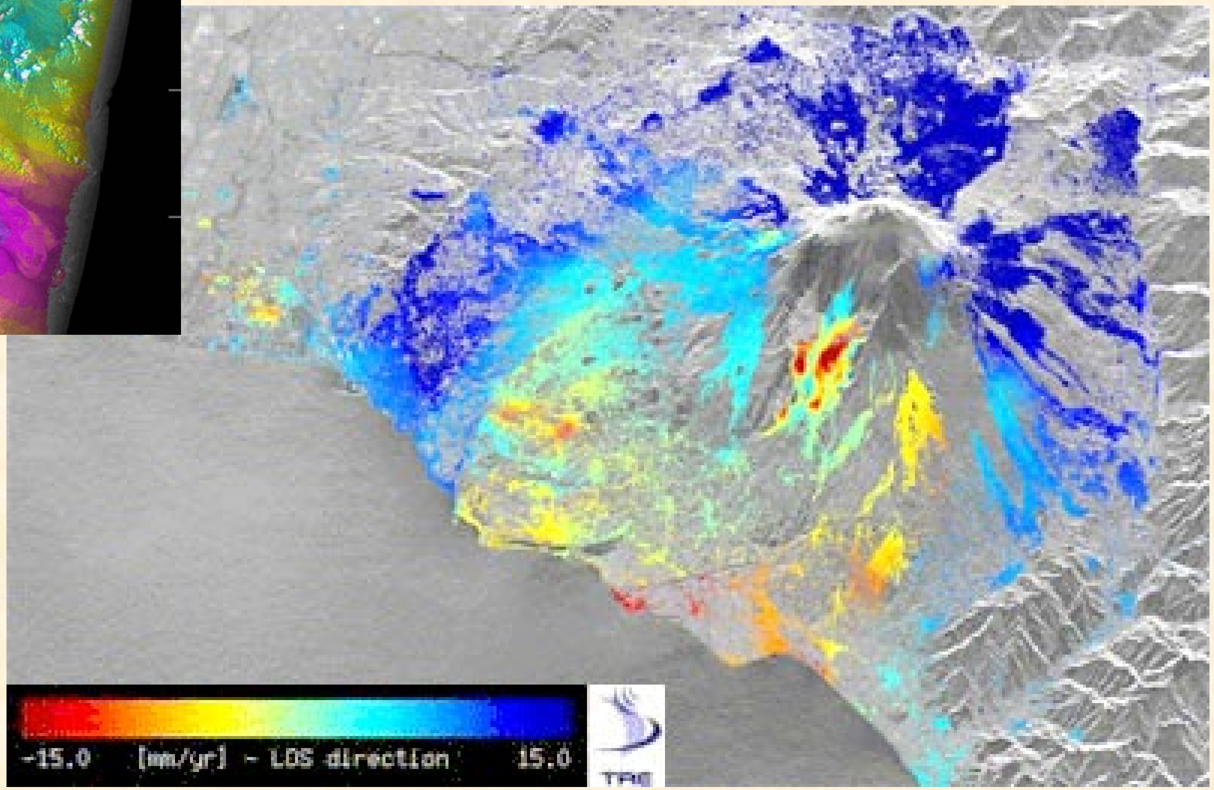

http://eopi.esa.int/esa/esa?type=upload&ts=1071071849723&table=result&cmd=image&id=128

"Differential Tomography"!

2D support in 2D Baseline-Time plane needed

Sparse 2D:
two-/multi-antenna
/sat. cluster
& multi-pass

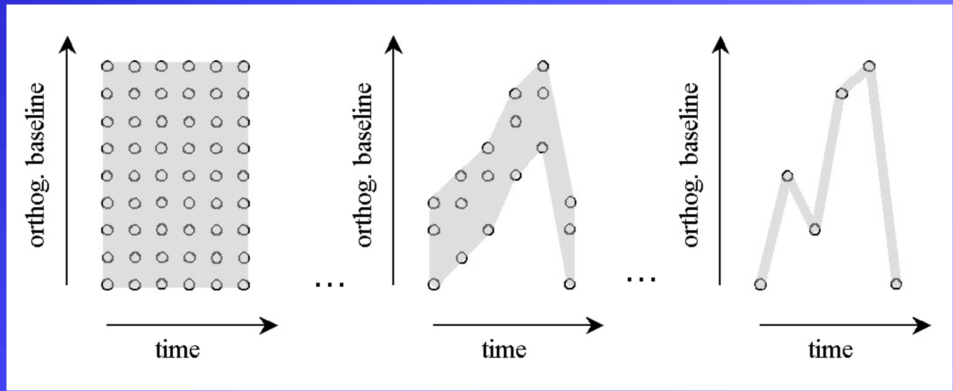

"1D" Curvilinear:
plain multi-baseline
by multi-pass,
airborne/sat.

Processing Framework

after registration, compensation of phase artifacts, deramping:

$$\mathbf{A}(\omega_S,\omega_T)=\begin{bmatrix} 1 & \cdots & e^{j[\omega_S B_\perp(1,N_P)+\omega_T t(N_P)]} \\ \vdots & \cdots & \vdots \\ e^{j\omega} \cdots & \cdots & \cdots \quad (N_P)] \end{bmatrix} \quad \cdots$$

Bidimensional Baseline-Time
Spectral Estimation !
$\mathbf{a}(\omega_S,\omega_T)$

z (3D) + Doppler resolution cell

Challenge: **Sparse Sampling** of 2D baseline-time support -
2D z-Doppler sidelobe problems to be attacked !

“4D Imaging”! (3D + T)

Simulated Bonn Data Set
ERS-1
10 passes
time span: 27 days
overall baseline: 1418 m

***SNR*=15, 12, 9 dB**
negligible baseline
and temporal decorrelation;
monotonic motion jitter.

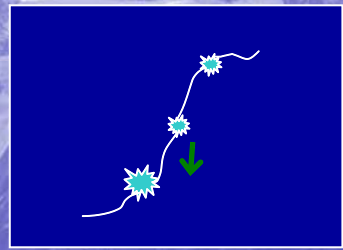

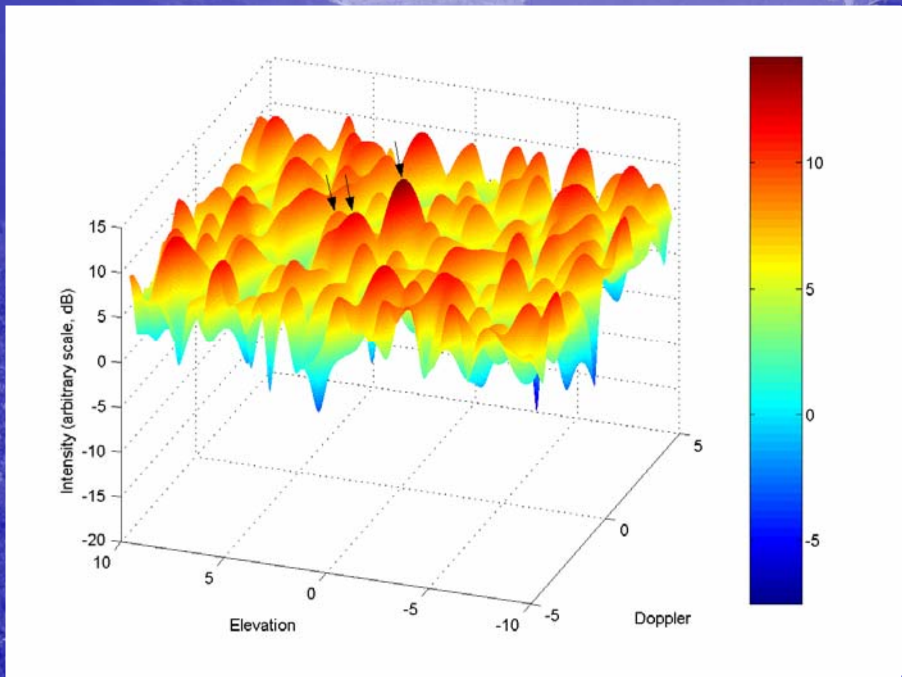

portion of Diff. + Tomo image

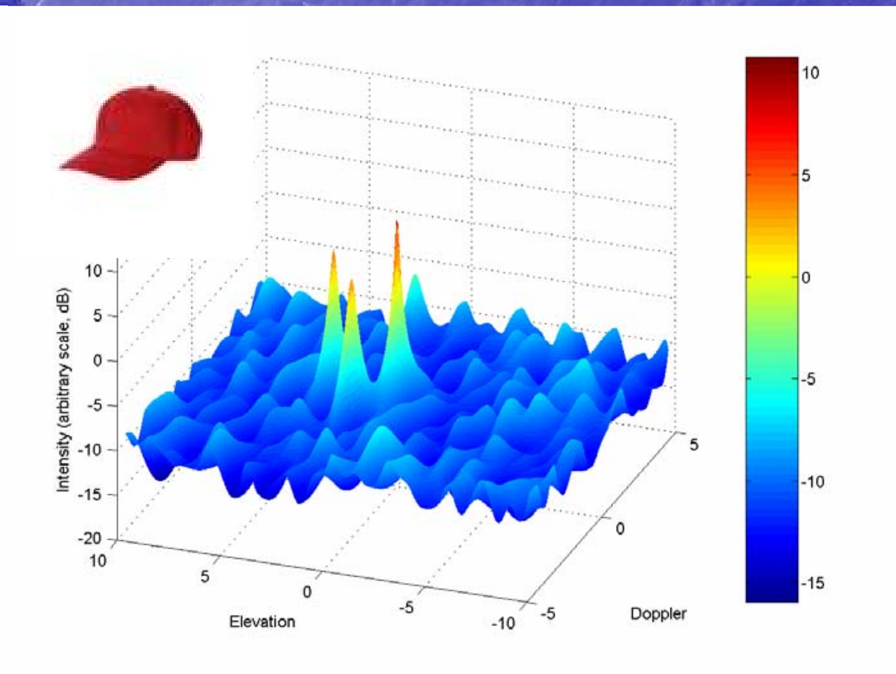

portion of Diff. + Tomo image

Results on real data of the ERS 1/2

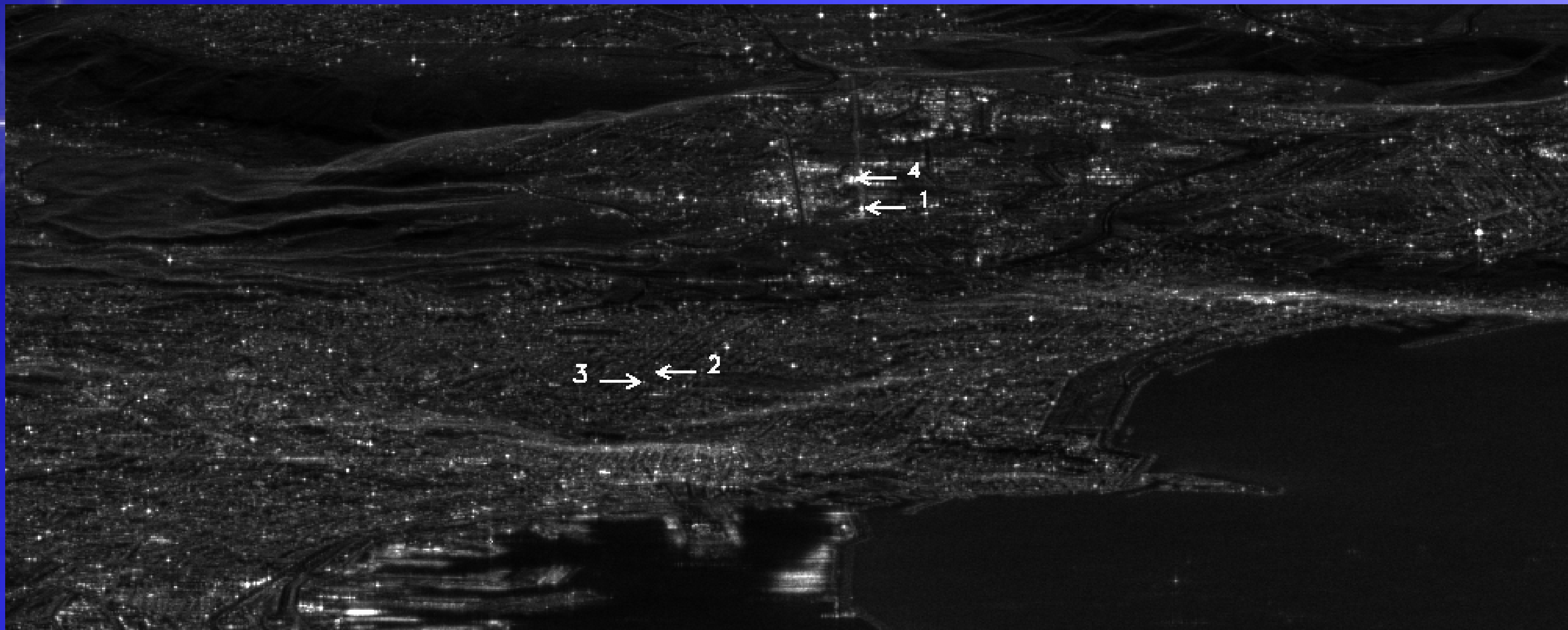

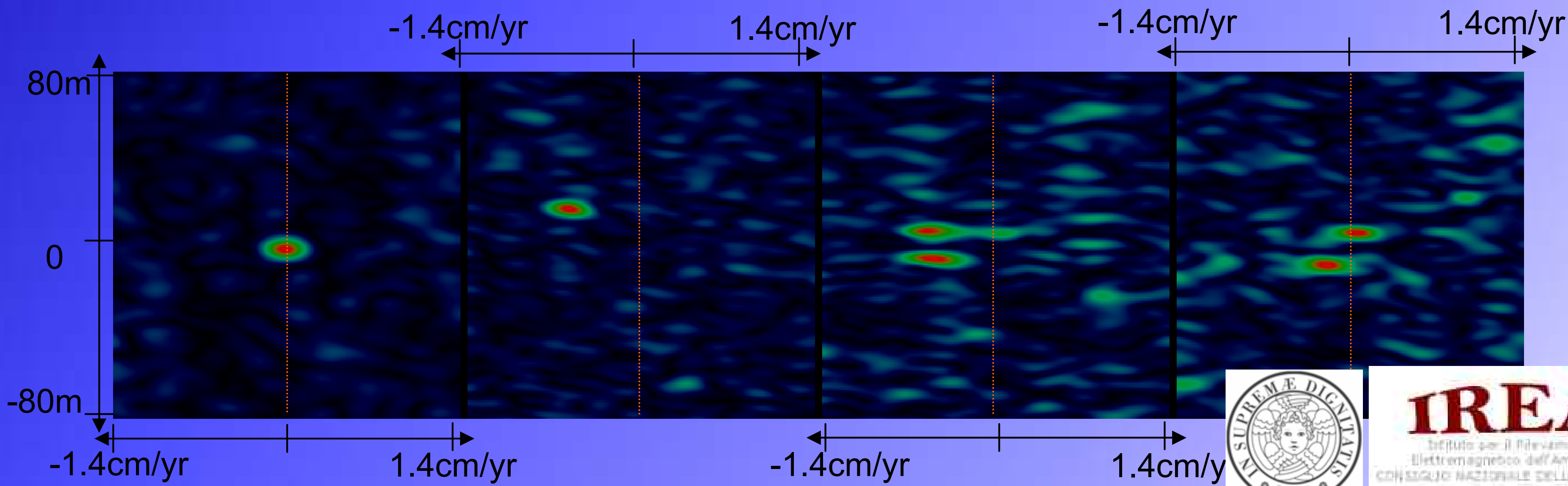

Results on real data of the ERS 1/2

- Single scatterers -

- Double scatterers -

LIMES
Land and Sea Integrated Monitoring for European Security

IREA
Istituto per il Rilevamento Elettromagnetico dell'Ambiente
CONSIGLIO NAZIONALE DELLE RICERCHE

TELESPAZIO
A Finmeccanica / Alcatel Company

“full 4D Imaging”! (continuous 3D + T)

Simulated Results

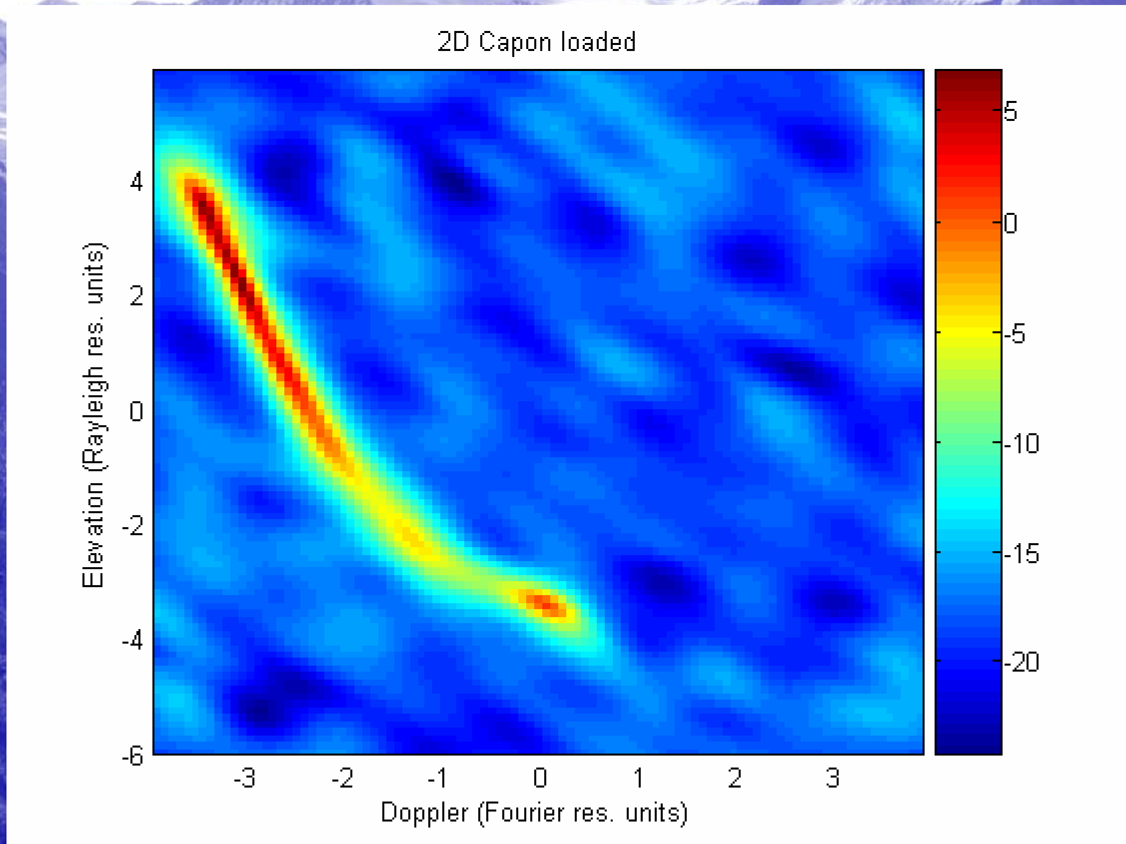

“Eco-Doppler” radar imaging of a glacier flow !

Interpolation of non-uniformly sampled data

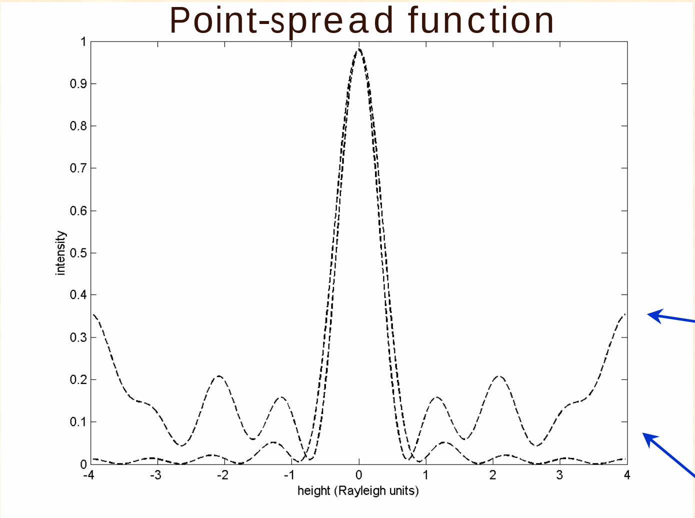

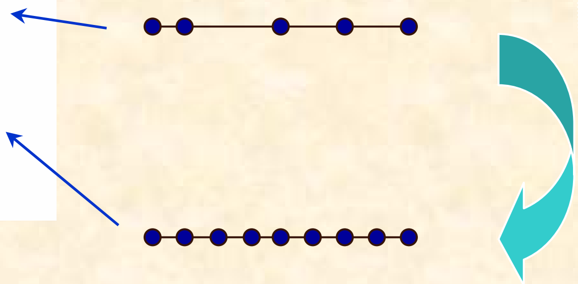

***A-priori information*:**
spectral support
(Sector of Interpolation)

Problema di "predizione"

The new interpolated approach

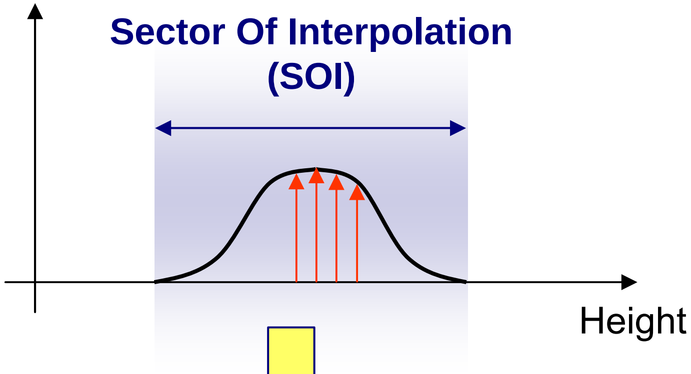

IDEA:

Reconstruct K_V uniform samples of the spatial harmonic of interest from the actual non-uniform samples

Non-uniform spatial sampling
***K* samples – real array**

Uniform spatial sampling
K_V samples – virtual array

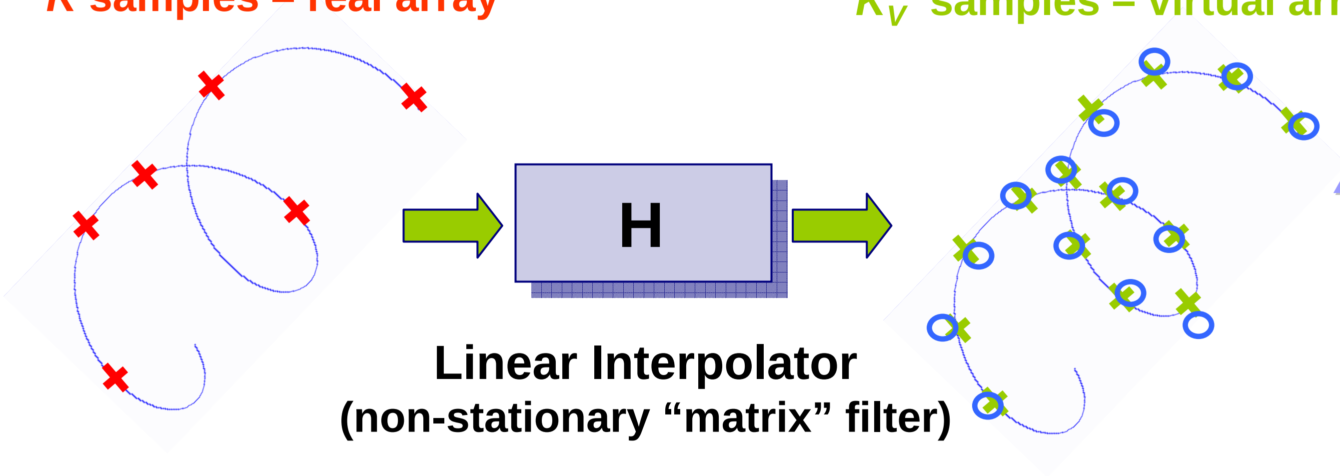

Linear Interpolator
(non-stationary "matrix" filter)

Apply this process for all the spatial harmonics inside the SOI!

Matrix filter principle

Moving window filter – One coefficient vector **h**
Linear, spatially stationary

Matrix filter – Coefficient vectors **$h_1, \ldots, h_N$**
Linear, spatially non-stationary

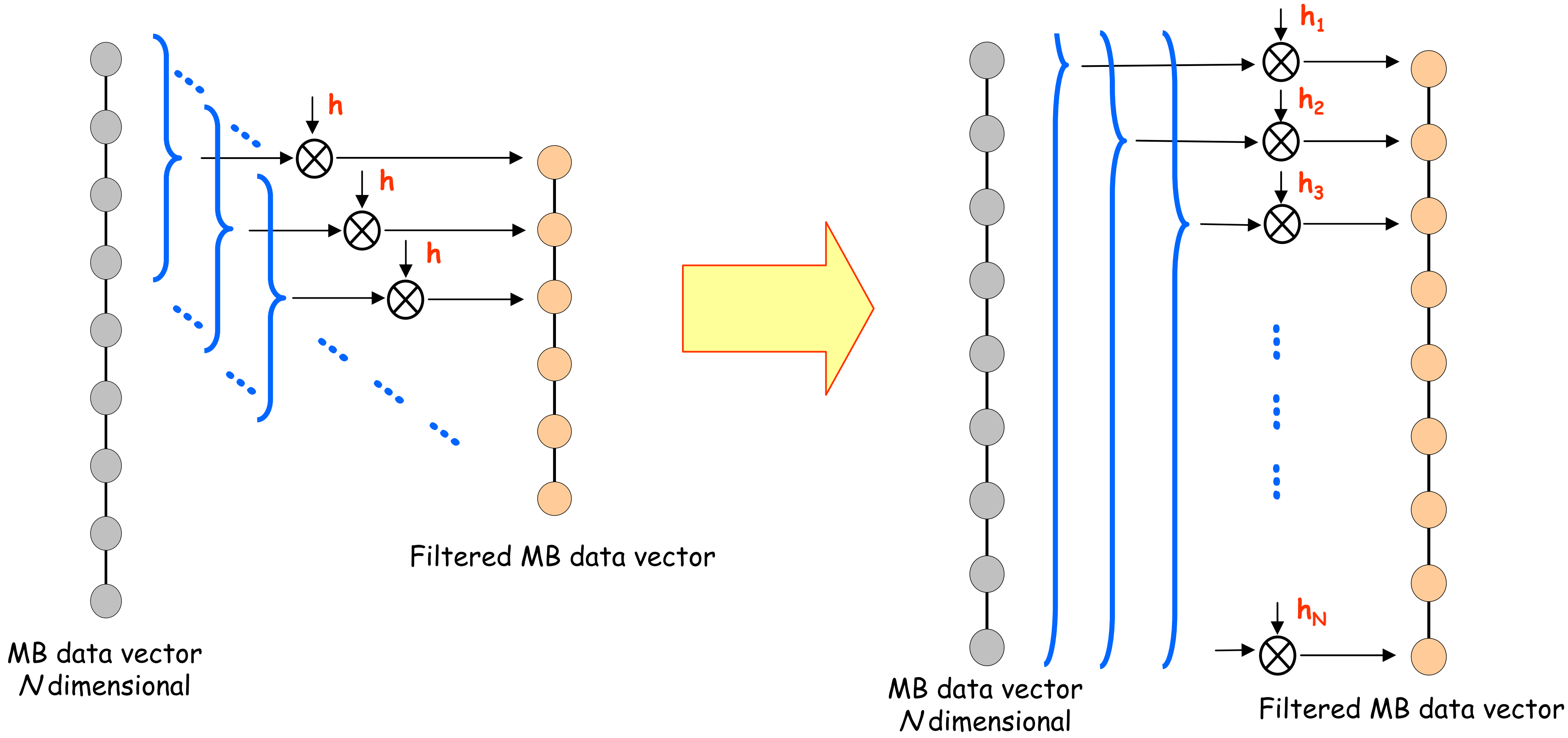

$\otimes$
inner product

- *Arbitrary input/output MB spacing allowed*

Array interpolation

Deterministic approach – IA

The output vector of the virtual array can be obtained by means of a $K_V \times K$ transformation matrix by solving the least squares (LS) problem:

$$\mathbf{H}_F = \arg\min_{\mathbf{H}} \left\| \mathbf{A}_V - \mathbf{H}\mathbf{A} \right\|_F^2$$

where

$$\mathbf{A}_V = [\mathbf{a}_V(\phi_1) \quad \mathbf{a}_V(\phi_2) \quad \cdots \quad \mathbf{a}_V(\phi_s)]$$
$$\mathbf{A} = [\mathbf{a}(\phi_1) \quad \mathbf{a}(\phi_2) \quad \cdots \quad \mathbf{a}(\phi_s)]$$

$[\phi_1 \ \phi_2 \ \ldots \ \phi_s]$ are s phase samples inside the discretized SOI.

Statistical approach – MSE-IA

The signal vector χ_{ULA} can be estimated minimizing the mean square error (MSE):

$$\mathbf{H}_M = \arg\min_{\mathbf{H}} E\left\{ \left(\chi_{ULA} - \mathbf{H}\mathbf{y} \right)^2 \right\}$$

This minimization (*Wiener-Hopf equations*) involves the knowledge of the spatial power spectral density, which can be assumed flat over the SOI in the InSAR application.

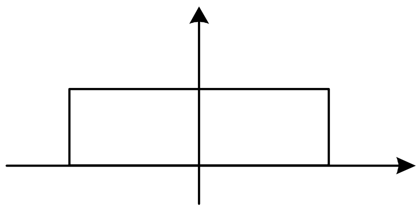

Costa Rica and Amazon Rainforest

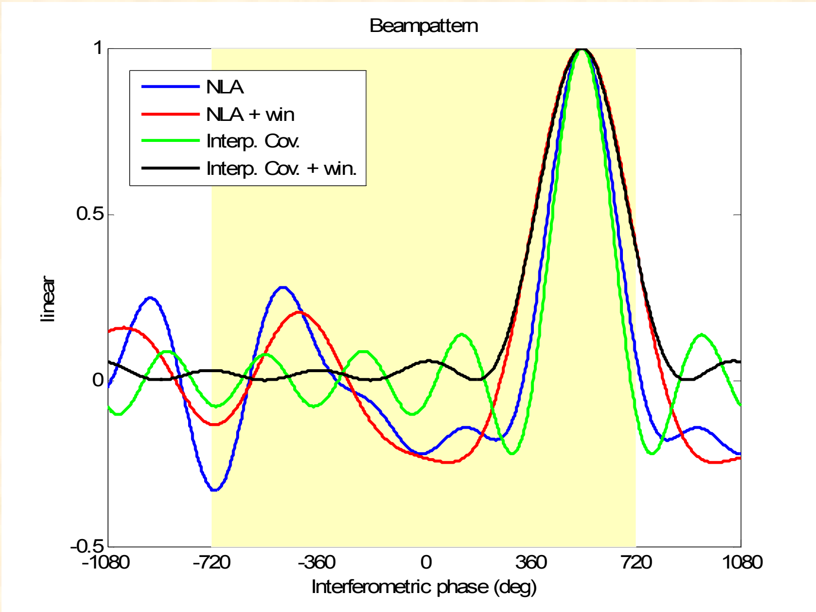

Jet Propulsion Laboratory
California Institute of Technology

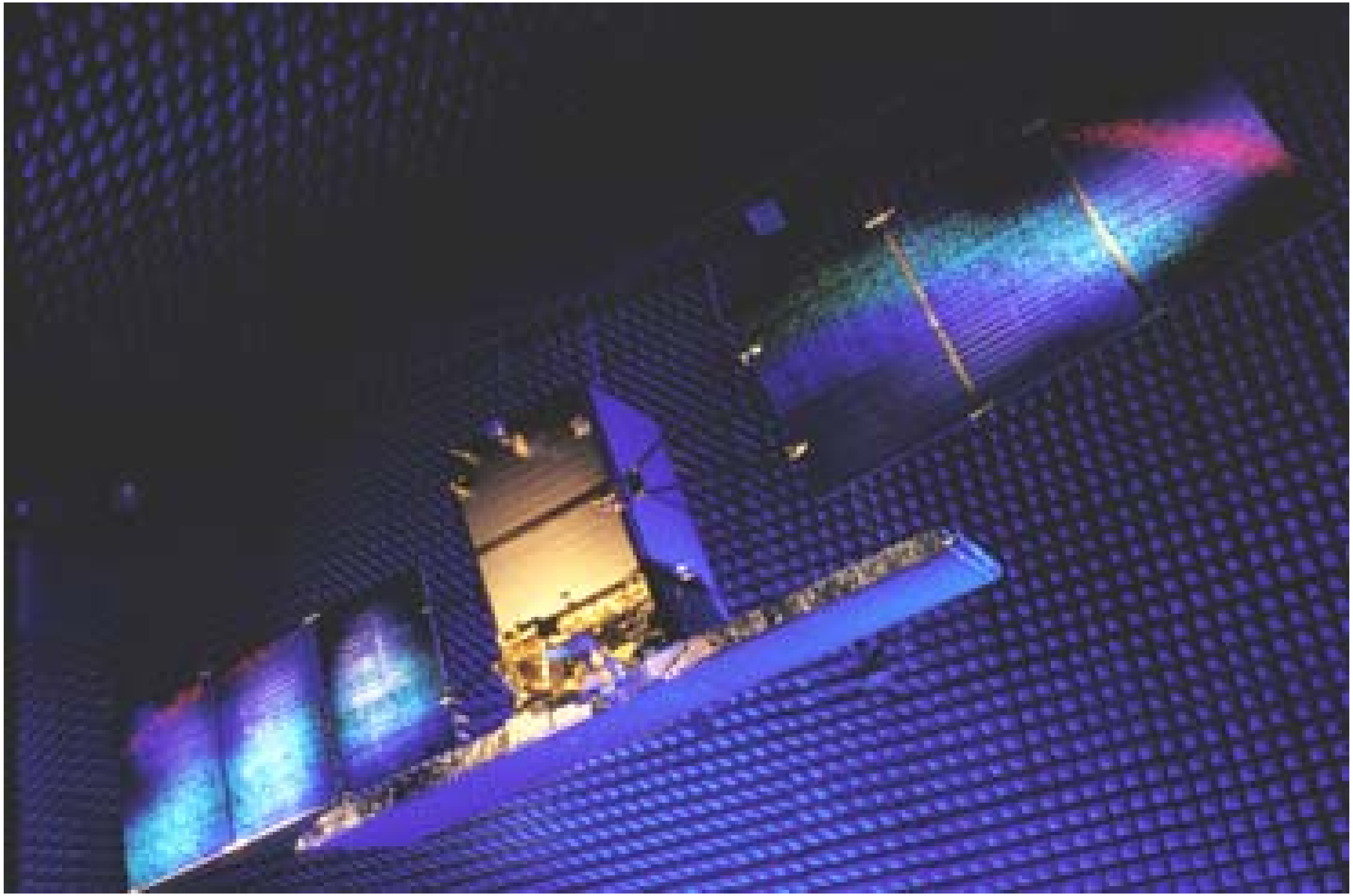

Il satellite italiano COSMO-SkyMed

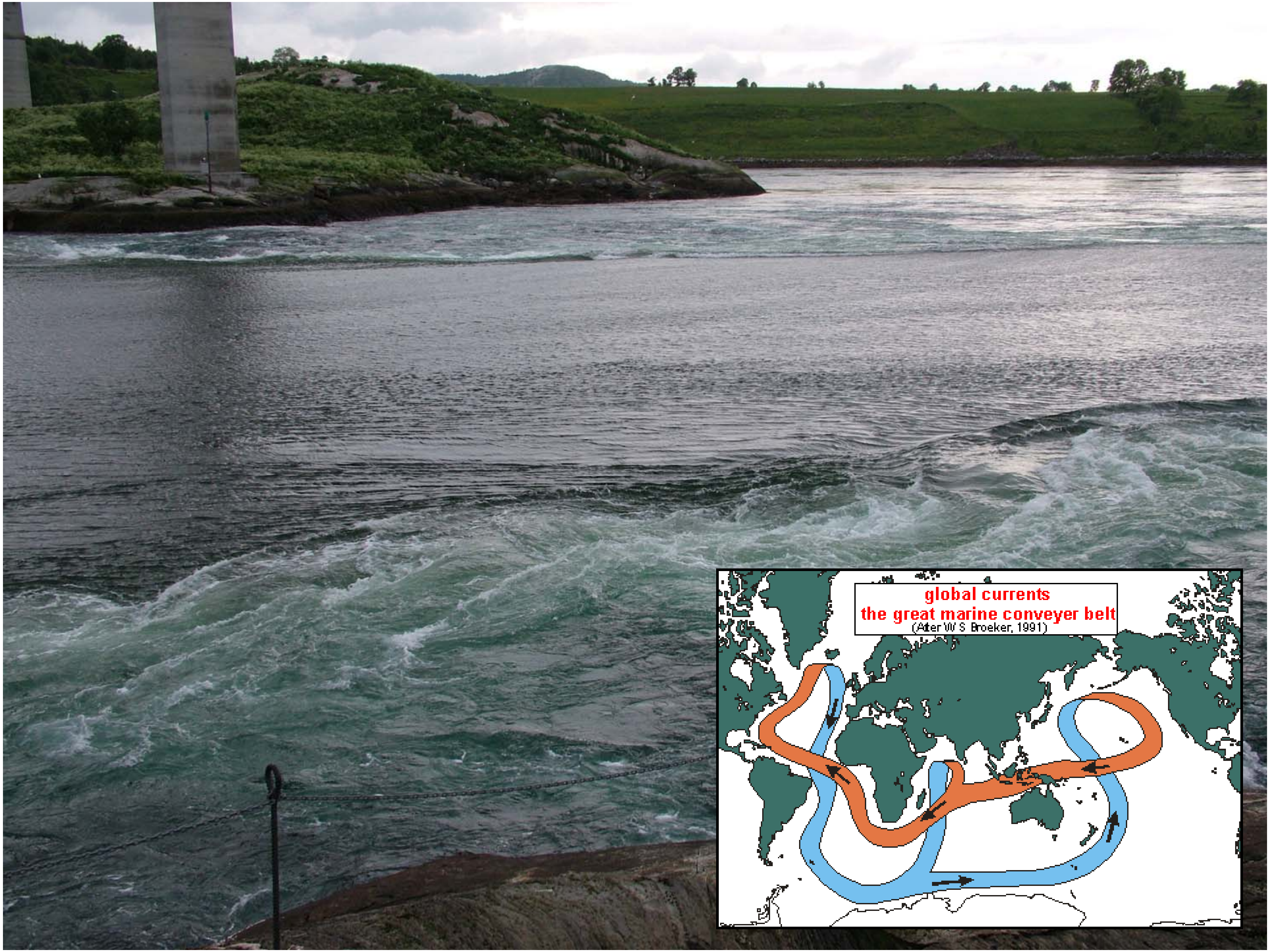
global currents
the great marine conveyer belt
(After W S Broeker, 1991)

Feasibility Study of Along-track SAR Interferometry with the COSMO-SkyMed Satellite System

Dept. of Ingegneria dell'Informazione, University of Pisa, via Caruso 14 - Pisa, Italy

Alenia Spazio – A Finmeccanica Company

In Supremae Dignitatis 1343

agenzia spaziale italiana

The Italian COSMO-SkyMed system

- 4-satellite constellation
- mapping of Mediterranean latitudes
- Hi-res X-band SAR
- Short revisit time

Along-Track Interferometry

- *ocean surface current velocity*
- ocean coherence time
- *sea waveheight spectrum*

and MTI

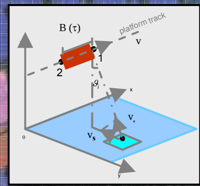

Spaceborne ATI

- NASA SRTM (along-track boom component)

TerraSAR-X split-antenna

RADARSAT-II (split-antenna MTI)

Satellite formations (distributed interferometers)

Performance study of *split-antenna* ATI modes for COSMO-Skymed SAR:

Statistical data model

multilook data vector (up to 5 rx channels: Multi Baseline ATI)

$$\mathbf{y}(n) = \sqrt{\sigma^2}\,\mathbf{A}(\varphi)\mathbf{x}(n) + \mathbf{v}(n)$$

speckle autocorrelation function

$$[\mathbf{C}_x]_{i,l} = \exp\left\{-\left(\frac{(l-i)\tau}{(K-1)\tau_c}\right)^2\right\}$$

data covariance matrix

$$\mathbf{R} = E\{\mathbf{y}(n)\mathbf{y}^H(n)\} = \sigma^2\mathbf{A}(\varphi)\mathbf{C}_x\mathbf{A}(\varphi)^H + \sigma_v^2\mathbf{I}$$

Cramér-Rao Lower Bound accuracy analysis

unknown and nuisance parameters $\boldsymbol{\chi} = [\varphi\ \tau_c\ \sigma^2\ \sigma_v^2]^T$

$CRLB(\chi_i) = [\mathbf{J}_{FIM}^{-1}]_{i,i}$ Fisher information

$$[\mathbf{J}_{FIM}]_{i,j} = N\,\mathrm{tr}\left\{\mathbf{R}^{-1}\frac{\partial\mathbf{R}}{\partial\chi_i}\mathbf{R}^{-1}\frac{\partial\mathbf{R}}{\partial\chi_j}\right\}$$

surface current velocity

$$v_s = \frac{\lambda v}{4\pi B\sin\vartheta_i}\varphi + v_B$$

Bragg velocity

accuracy of conventional 2-ch. ATI

$$\mathrm{CRLB}^{1/2}(v_s) = \frac{\lambda v}{4\pi B\sin\vartheta_i}\frac{1}{\sqrt{2N}}\frac{\sqrt{1-(\rho_s\rho_t)^2}}{\rho_s\rho_t}$$

System and physical models

SAR equation for extended targets, split antenna

Moore and Fung ocean scattering model

$$\sigma^0(\phi_{az},\vartheta_i,u_w) = [A + B\cos\phi_{az} + C\cos 2\phi_{az}]\,e^{-(\vartheta_i-\bar\vartheta)/\vartheta_0}\left(\frac{u_w}{\bar u_w}\right)^\gamma$$

coherence time model (Frasier and Camps)

$$\tau_c = 3\frac{\lambda}{u_w}erf^{-1/2}\left(2{,}7\frac{r_g}{u_w^2}\right)$$

Platform velocity	7548 m/s
Slant range distance	732 Km
Antenna length	5.6 m
Carrier frequency	9.58 GHz
Incidence angle	25°-50°
TX peak power	5 KW
Bandwidth	99.3 MHz

A few split mode configurations:	*# rx panels per ch.*	*# ch.*	*B [m]*
STTX+SPAN2a	1	2	2.24
STTX+SPAN2b	2	2	1.68
STTX+SPAN2c	3	2	1.12
STTX+SPAN3d	3	3	1.12

Investigated trade-offs

- baseline length
- sub-aperture gain
- channel number
- speckle decorrelation

azimuth ambiguity

Conv. and MB coherence time estimation and quantization effects also investigated

Rankings

1° STTX+SPAN4/SPAN5
2° STTX +SPAN2b
3° STTX +SPAN2a/SPAN3a
4° STTX +SPAN2c/3d

A few results:

Signal level

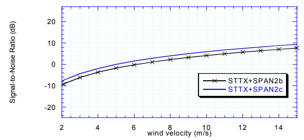

cross-wind, mid-range, r_g=2.7 m

Coherence time

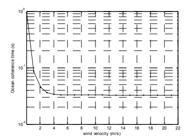

up- and down-wind

Velocity accuracy

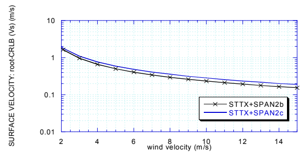

down-wind, N=1000 looks

Resolution

	Accuracy=10 cm/s, mid-range	Accuracy=25 cm/s, mid-range	Accuracy=25 cm/s, far-range
STTX+SPAN2b	N=189035 ATI cell=1271 m	N=30245 ATI cell =508 m	N=50592 ATI cell =657 m
STTX+SPAN2c	N=235683 ATI cell =1419 m	N=37709 ATI cell =568 m	N=58602 ATI cell =708 m

cross-wind

Lancio del satellite italiano COSMO-SkyMed (COSMO-1, Giugno 2007)

COSMO-SkyMed/BISSAT cluster

ATI Sea Currents and Waves

- Cramér-Rao bound analysis on the expected precision on surface current velocity estimation
- SAR equation for extended target
- Physical models for ocean scattering and coherence time (τ_c)

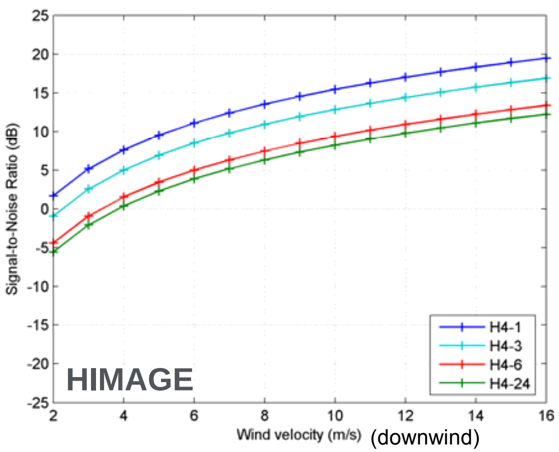

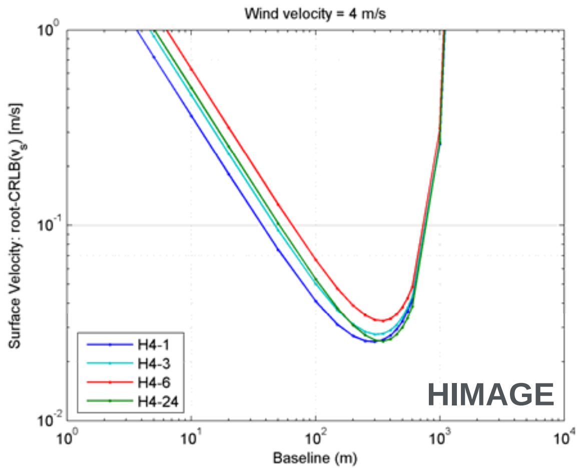

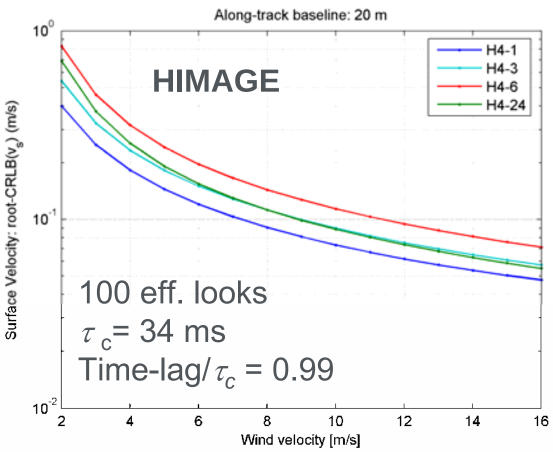

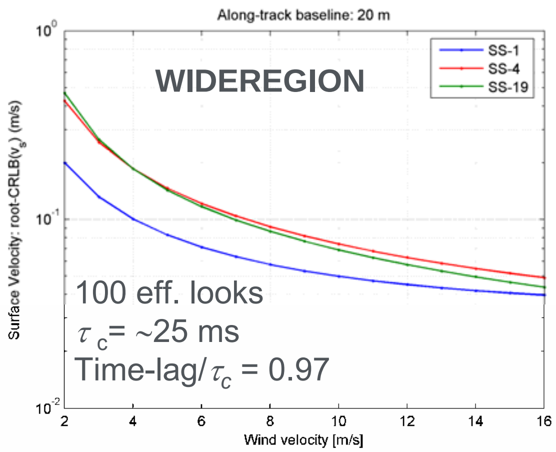

- A rescaling of the number of looks is evaluated to obtain the desired precision (≤0.1 m/s at worst)
- @ B_{ATI}=20 m, =~0.1 m/s absolute surface velocity accuracy is obtained with B_{XTI}<500 m (availability of precise radar altimer oceanographic data and DEM of a terrain zone in the image)

Possible extension: *BISSAT with COSMO-SkyMed in split-antenna mode*

- Dual baseline system
- Small baseline: enlargement of the velocity ambiguous range
- Long baseline: augmented interferometric sensitivity, eased absolute calibration

Example: 200 m total baseline, 3.36 m small baseline (STTX-SPAN2b): higher multilooking degree (50 instead of 15 in the single baseline case) to ensure the desired precision of 0.1 m/s

System model perturbations

Residual multibaseline array calibration or atmospheric compensation errors affect the data in all the practical applications

Phase error vector introduced by the residual miscalibration at each array phase center:

$$\mathbf{e} = \begin{bmatrix} e^{j4\pi d_1} & e^{j4\pi d_2} & \dots & e^{j4\pi d_K} \end{bmatrix}^T$$

$d_1 \dots d_K$ **Gaussian, zero mean, uncorrelated random variables, with variance σ^2**

- **Positioning errors** of the array elements (normalized to wavelength), due to uncertainties in the platform positioning in the direction parallalel to the line of sight (errors in the perpendicular direction can be neglected)
- **Residual one-way path delay** variations of wave propagation through the atmosphere (normalized to wavelength)

Total array response: $\mathbf{a}(h) = \mathbf{a}_P(h) \odot \mathbf{e}$

Element-by-element product

Hybrid Cramér-Rao Bound

Speckle vector (multiplicative noise)

Signal model:
$$\mathbf{y}(n) \approx \sum_{i=1}^{N_S} \sqrt{\tau_i}\,\mathbf{a}_P(\varphi_i) \odot \mathbf{e} \odot \mathbf{x}_i(n) + \mathbf{v}(n) \qquad n = 1, 2, \ldots, N$$

K = # of array elements
N_S = # of sources

Steering vector

Calibration error vector

Cramér-Rao bound

$$\xi = \begin{bmatrix} \varphi_1 & \cdots & \varphi_{N_S} & \tau_1 & \cdots & \tau_{N_S} & b_1 & \cdots & b_{N_S} & \sigma_V^2 \end{bmatrix}^T$$

Parameter vector

$$\left[\mathbf{J}_{FIM}\right]_{m,n} = -\mathrm{E}_{\mathbf{y}}\left\{\frac{\partial^2 \ln\left(\iint \ldots \int f(\mathbf{y},\mathbf{e};\xi)\,\mathrm{d}d_1 \mathrm{d}d_2 \ldots \mathrm{d}d_K\right)}{\partial \xi_m \partial \xi_n}\right\} \Rightarrow$$

Unfeasible !

Hybrid Cramér-Rao bound

Good trade-off between easiness of calculation and tightness

$$\xi = \begin{bmatrix} \varphi_1 & \cdots & \varphi_{N_S} & \tau_1 & \cdots & \tau_{N_S} & b_1 & \cdots & b_{N_S} & \sigma_V^2 & d_1 & \cdots & d_K \end{bmatrix}^T$$

Nuisance parameters

$$\left[\mathbf{J}_{H-FIM}\right]_{m,n} = -\mathrm{E}_{\mathbf{y},\mathbf{d}}\left\{\frac{\partial^2 \ln f(\mathbf{y},\mathbf{e};\xi)}{\partial \xi_m \partial \xi_n}\right\} = -\mathrm{E}_{\mathbf{d}}\left\{\mathrm{E}_{\mathbf{y}|\mathbf{d}}\left\{\frac{\partial^2 \ln f(\mathbf{y},\mathbf{e};\xi)}{\partial \xi_m \partial \xi_n}\right\}\right\} \Rightarrow HCRB(\xi_k) = \left[\mathbf{J}_{H-FIM}^{-1}\right]_{k,k}$$

System model perturbations: *Hybrid CRLB*

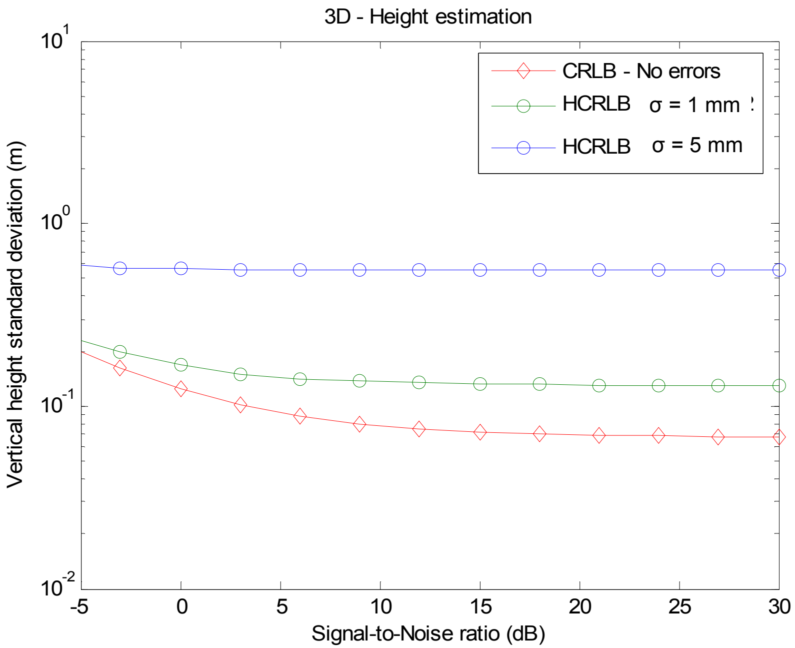

3D: height

Double scatterer distance in height: 2 r.u.

Notes:

- σ is standard deviation of residual atmospheric one-way path delay variations
- Variations uncorrelated from track to track
- Compensated l.o.s. velocity

Robust interpolator derivation

Again: $$\mathbf{y}_V(n) = \mathbf{H}_I \mathbf{y}(n)$$

Robust interpolator, $K_V \times K$ matrix

In the perfectly calibrated case: $$\mathbf{H}_I \mathbf{A}_P = \mathbf{A}_{P,V}$$

Overdetermined equation system: LS solution

NLA array steering matrix: *The columns are the NLA st. vectors calculated for a number of spatial frequency in the SOI*

Virtual array steering matrix: *The columns are the virtual st. vectors calculated for the same spatial frequencies in the SOI*

In the presence of calibration errors:

$$\mathbf{H}_I \left(\mathbf{A}_P + \mathbf{\Delta A}_P \right) = \mathbf{A}_{P,V} + \mathbf{\Delta A}_{P,V}$$

Calibration error

Interpolation error

$$\boxed{\mathbf{H}_I = \arg\min_{\mathbf{H}} E\left\{ \left\| \mathbf{\Delta A}_{P,V} \right\|_F^2 \right\}}$$

LS solution to a perturbed equation system

Results of the robust processing

K = 24 highly non uniform, K_V = 29
σ = 0.01 (λ units)

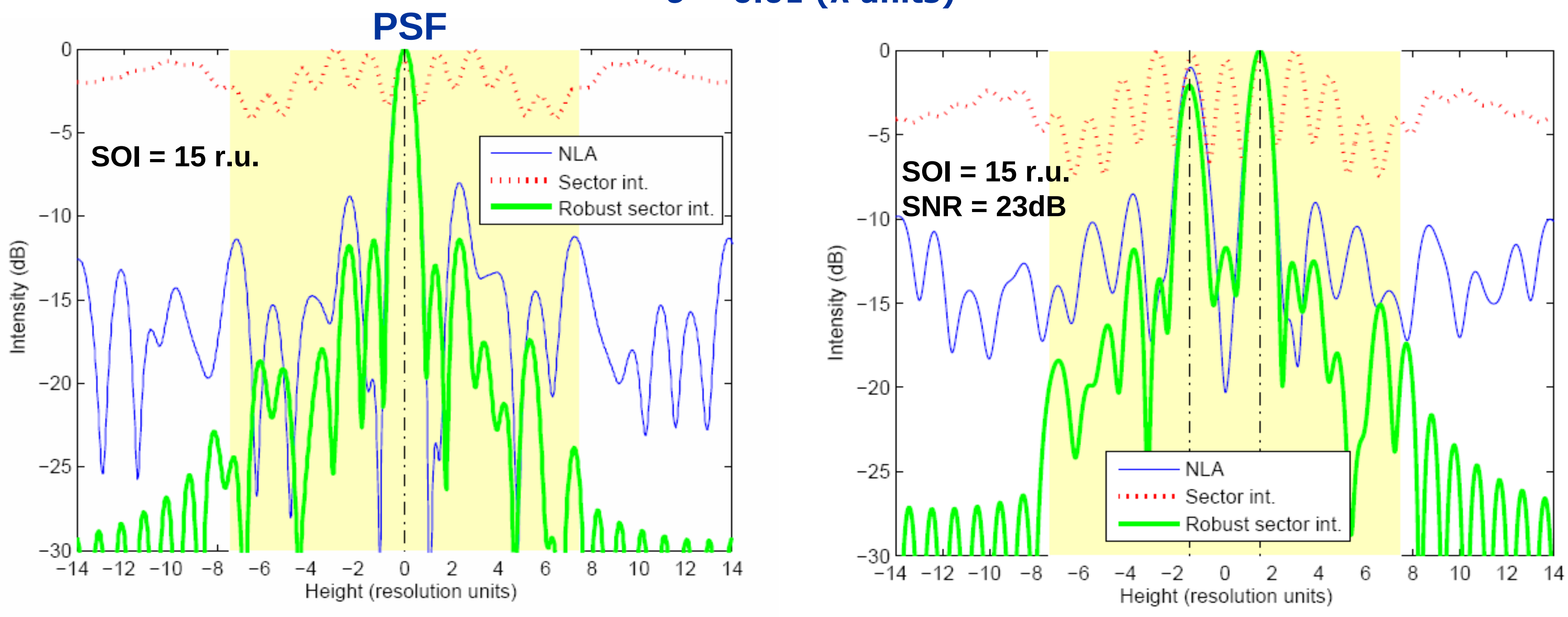

- **The basic sector interpolator degrades in the reconstruction of the tomographic profile**
- **The higher effectiveness of the robust method is apparent**